



**TRIBHUVAN UNIVERSITY
INSTITUTE OF ENGINEERING
PULCHOWK CAMPUS**

THESIS NO.: M-130-MSESPM-2017-2021

**Pelton Runner Erosion Due To Cavitation : A Case Study Of Storage
Hydropower Plant, Kulekhani First Hydropower Station.**

by

NARENDRA KUMAR MANDAL

A THESIS

**SUBMITTED TO THE DEPARTMENT OF MECHANICAL AND
AEROSPACE ENGINEERING IN PARTIAL FULFILLMENT OF THE
REQUIREMENTS FOR THE DEGREE OF MASTER OF SCIENCE IN
ENERGY SYSTEM PLANNING AND MANAGEMENT**

**DEPARTMENT OF MECHANICAL AND AEROSPACE ENGINEERING
LALITPUR, NEPAL**

SEPTEMBER, 2021

The author has agreed that the library, Department of Mechanical and Aerospace Engineering, Pulchowk Campus, Institute of Engineering may make this thesis freely available for inspection. Moreover, the author has agreed that permission for extensive copying of this thesis for scholarly purpose may be granted by the professor(s) who supervised the project work recorded herein or, in their absence, by the Head of the Department wherein the thesis was done. It is understood that the recognition will be given to the author of this thesis and to the Department of Mechanical and Aerospace Engineering, Pulchowk Campus, Institute of Engineering in any use of the material of this thesis. Copying or publication or other uses of this thesis for financial gain without approval of the Department of Mechanical and Aerospace Engineering, Pulchowk Campus, Institute of Engineering and author's written permission is prohibited.

Request for permission to copy or to make any other use of the material in this report in whole or in part should be addressed to:

Head

Department of Mechanical and Aerospace Engineering

Pulchowk Campus, Institute of Engineering

Lalitpur, Kathmandu

Nepal

TRIBHUVAN UNIVERSITY
INSTITUTE OF ENGINEERING
PULCHOWK CAMPUS

DEPARTMENT OF MECHANICAL AND AEROSPACE ENGINEERING

The undersigned certify that they have read, and recommend to the Institute of Engineering for acceptance, a thesis entitled “**Pelton runner erosion due to cavitation: A case study of storage hydropower plant, Kulekhani first hydropower station**” submitted by Narendra Kumar Mandal in partial fulfilment of the requirements for the degree of Master in Energy System Planning and Management.

Supervisor, Dr. Tri Ratna Bajracharya
Professor, Department of Mechanical and Aerospace
Engineering, Pulchowk Campus, IOE

Supervisor, Dr. Hari Bahadur Darlami
Assoc. Professor, Department of Mechanical and
Aerospace Engineering, Pulchowk Campus, IOE

External Examiner, Er. Dharendra Chaudhary
Manager, Nepal Electricity Authority
Kulekhani First Hydropower Station, Dhorsing,
Makawanpur

Committee Chairperson, Dr. Surya Prasad Adhikari
Head, Department of Mechanical and Aerospace
Engineering, Pulchowk Campus, IOE

Date: 15 September 2021

ABSTRACT

Storage Hydropower Plants with reservoir are more flexible and reliable than the Run-off River Plants. It actually acts as battery bank or power bank for desire power generation for uncertain demand. Kulekhani First Hydropower Station is only one storage type hydropower station in Nepal. It is 60 MW plant and is very reliable power plant of Nepal. Electricity produced from each m^3 of reservoir water is calculated as 1.27 kWh. Measurements & sedimentation data from the primary and secondary sources were taken for analysis. Trend lines and bar charts were used for analysis purpose.

This study is an attempt to find out that Pelton runner erosion due to cavitation phenomena along with efficiency deterioration, though it operates under atmospheric pressure, where sediment concentration is quite low. This was found from the case study of storage hydropower plant, Kulekhani First Hydropower Station. Sediment analysis were carried out on laboratory as per the guidelines of International Electro-Technical Commission (IEC) 62364. The laboratory Test report informs that the sediment concentration of reservoir water feeding to turbine is quite low i.e. 70 ppm. Also the major mineral contents are Quartz, Feldspar, Mica and Other (Tourmaline, Homblende, Calcite, Clay, Hard rock fragments, clay lumps etc.). Sizes of mineral content ranges from 0.001 to 1mm. The result of the study clearly shows that cavitation do occur, though it operates under atmospheric condition. The Pelton runner erosion due to cavitation occurs mainly at the splitter tip back side zone and gradually increasing on operation basis. Erosion contribution due to cavitation is about 0.5045 mm/year whereas erosion contribution due to sand particle is about 0.0046 mm/year. Also the study reveals that the plant efficiency has a degrading trend line along with fluctuations. The efficiency calculation are done on the basis of daily water consumption and fluctuating effective head where water volume is determined with polynomial based reservoir capacity equation.

ACKNOWLEDGEMENTS

I sincerely thank all the people who provided the assistance, encouragement and constructive criticism leading to the completion of this thesis. I would like to express my gratitude to the Department of Mechanical and Aerospace Engineering, Institute of Engineering, Tribhuvan University for providing me an important platform to materialize out engineering knowledge gained during masters program.

A perfect guidance with regular encouragement from my thesis supervisor Dr. Tri Ratna Bajracharya, Professor and Dr. Hari Bahadur Darlami, Associate Professor, Department of Mechanical and Aerospace Engineering has made me indebted.

Besides my supervisor, I would like to thank Dr. Nawraj Bhattarai, Associate Professor, Program Coordinator of Energy system planning and management (MSESPM), for encouragement and insightful comments. Departmental Head Dr. Surya Prasad Adhikari, Associate Professor for proper informations from department, Dr. Laxman Poudel, Professor, Co-ordinator of Mechanical system design and engineering for valueable suggestions. Hari Bahadur Dura, Assistant Professor and Bijendra Prajapati, Assistant Professor for guidance in report writing & formating with relevant sugestions and tips.

I express my humblest gratitude to Plant Manager , Civil Engineer Gopal Prasad Gupta, Mechanical Engineer Shiva Kumar Thapa, Mechanical Assistant Engineer Vishm Raj Chaudhary, Store Incharge Suman Shiwakoti, Electrical Foreman Suvash Pudasaini, Shushma Tiwari, Mechanical Helper Bisnual Mijar, Bhuwan Gole and all staffs of Kulekhani First Hydropower Station who helped me in providing necessary data and suggestions and supporting in my thesis related works.

I am very thankful to my Engineer friends Puran Sob, Pradeep Singh, Ashesh Babu Timilsina, Aprin Bajracharya, Niroj Dahal, Ramesh Shrestha, Suman Manandhar, Sudip Shiwakoti, Nivesh Karna, and Hari Dhakal for their support, help and encouragement in each and every steps of my thesis works.

Finally, I would like to acknowledge with gratitude, the continuous support and love of my family - my wife, Babita; my son, Basant. Their continuous help and encouragement had always inspired me for my thesis works.

TABLE OF CONTENTS

COPYRIGHT.....	I
ABSTRACT.....	IV
ACKNOWLEDGEMENTS.....	V
TABLE OF CONTENTS.....	2
LIST OF ABBREVIATIONS.....	4
LIST OF TABLES.....	5
LIST OF FIGURES.....	6
1 CHAPTER ONE: INTRODUCTION.....	7
1.1 Background.....	7
1.1.1 Kulekhani First Hydropower Station, NEA.....	9
1.1.2 Active and dead volume of reservoir.....	12
1.1.3 Elevation-Reservoir capacity:.....	13
1.1.4 Reservoir inflow.....	14
1.1.5 Turbines.....	14
1.1.6 Plant efficiency.....	17
1.2 Problem statement.....	18
1.3 Objectives.....	18
1.4 Assumptions and limitations.....	19
2 CHAPTER TWO: LITERATURE REVIEW.....	20
2.1 Theory of Pelton Turbine.....	20
2.2 Erosion in turbine.....	21
2.3 Cavitation phenomena.....	23
2.4 Computational Fluid Dynamics.....	25
2.4.1 Pre-Processor.....	26
2.4.2 Solver.....	26
2.4.3 Post-Processor.....	26
2.5 The finite volume method.....	27
2.5.1 Continuity and Navier-Stokes Equation.....	27
2.5.2 Turbulence Modelling.....	27
2.6 Past research done on erosion of Pelton turbine.....	28
3 CHAPTER THREE: RESEARCH METHODOLOGY.....	34
3.1 Literature Review.....	35
3.2 Data Collection.....	35
3.3 Sediment concentration.....	36

3.4	Mineral Content	36
3.5	Particle size distribution.....	37
3.6	Technical observations.....	37
3.7	Computational model development for Pelton runner bucket	40
3.8	CFD Model Formulation.....	40
3.9	Estimations.....	41
4	CHAPTER FOUR: RESULTS AND DISCUSSION	42
4.1	Generation record of KL1HPS.....	42
4.2	Annual generation and water level of KL1HPS	42
4.3	Annual reservoir water level of KL1HPS	43
4.4	Efficiency calculations.....	44
4.5	Efficiency trend line.....	44
4.6	Volume of water outflow during machine operations	45
4.7	Volume of water inflow during machine stop	45
4.8	Measurements	46
4.9	Wear calculations of bucket profile	47
4.10	Erosion analysis	48
4.11	Comparison of sand led and sand free flow in Pelton turbine	48
4.12	CFD Modelling	49
5	CHAPTER FIVE: CONCLUSIONS AND RECOMMENDATIONS	51
5.1	Conclusions.....	51
5.2	Recommendations.....	51
	REFERENCES	52
	APPENDIX A: TABLES OF CHAPTER FOUR.....	55
	APPENDIX B: DRAWING OF PELTON RUNNER BUCKET	94
	APPENDIX C: LABORATORY TEST REPORT.....	97

LIST OF ABBREVIATIONS

FY	Fiscal Year
GW	Gigawatt
GWh	Gigawatt Hour
HPP	Hydro Power Project
HPS	Hydro Power Station
IEC	International Electrotechnical Commission
PPM	Parts Per Million
KL1HPS	Kulekhani First Hydropower Station
kW	Kilowatt
kWh	Kilowatt Hour
Mm ³	Million Meter Cube
MW	Megawatt
MWh	Megawatt Hour
NEA	Nepal Electricity Authority
NRs.	Nepali Rupees
PPA	Power Purchase Agreement
ROR	Run Off River
TWh	Terawatt Hour

LIST OF TABLES

Table 1.1: Classification of river sediment	8
Table 1.2: Salient features of Kulekhani First HPS	10
Table 1.3: Kulekhani reservoir features	13
Table 1.4: Feature of turbine of KL1HPS	15
Table 3.1: Sediment concentration of Kulekhani First HPS feed water	36
Table 3.2: Mineral content in Kulekhani First HPS feed water	37
Table 3.3: Overview of the basic setup	41
Table 4.1: Unit-2 Runner bucket (measurement)	47
Table 4.2: Theoretical calculations	47
Table 5.1: Annual generation of KL1HPS	56
Table 5.2: Annual generation and water level of KL1HPS	58
Table 5.3: Efficiency spreadsheet	61
Table 5.4: Volume of water outflow during machine operations	74
Table 5.5: Volume of water inflow during machine stop	83

LIST OF FIGURES

Figure 1.1: Kulekhani reservoir location	11
Figure 1.2: Quartz content in Nepalese rivers	12
Figure 1.3: Kulekhani reservoir with sloping intake	12
Figure 1.4: Active and dead volume of reservoir	13
Figure 1.5: Pelton runner bucket.....	15
Figure 1.6: Pelton runner of KL1HPS	17
Figure 2.1: Parts of a Pelton Turbine	20
Figure 2.2: Working of the Pelton turbine	21
Figure 2.3: Eroded Pelton turbine components.....	22
Figure 2.4: Saturation pressure against temperature (of Water)	23
Figure 2.5: Phenomenon of cavitation	24
Figure 2.6: Water jet	24
Figure 3.1: Research methodology chart	34
Figure 3.2: Erosion due to sand particle and cavitation (left Puwakhola HPS) and erosion due to cavitation (right KL1HPS) in bucket.....	38
Figure 3.3: After few years run minor effect of cavitation	39
Figure 3.4: On long run, tip erosion due to cavitation	39
Figure 4.1: Annual generation since commissioning till FY2077/78	42
Figure 4.2: Generation and water level chart.....	43
Figure 4.3: Annual max. & min. reservoir water level of KL1HPS	43
Figure 4.4: Efficiency deterioration trend line.....	44
Figure 4.5: Reservoir outflow to turbine.....	45
Figure 4.6: Volume of water inflow to reservoir	46
Figure 5.1: Drawing of Pelton runner bucket	95
Figure 5.2: Nozzle and Needle.....	96

CHAPTER ONE: INTRODUCTION

1.1 Background

Hydropower simply is a renewable source of energy. In hydropower system the potential energy of water is converted into kinetic energy which later converted in mechanical energy and finally into electrical energy. Hydropower is a traditional way of harnessing power or energy from water. In ancient period water mill's rotatory wheel were made to rotate with the power of running or falling water to crush the grain for livelihood. In doing so actually hydraulic energy of water were converted into mechanical energy and limited to it.

In modern era, with gradual development in human civilization as well as advancement in science and technology, not only the hydraulic energy of water was converted into mechanical energy instead electrical energy as well as further uses of water energy like steam from water to run gas turbine, heat energy form water for boiler operation etc. and many more day by day. Naturally Nepal is rich in water resource and poses hydropower potential of 83,000 MW theoretically and out which only 45,000 MW is techno-economically feasible. Presently about 2.3% of techno-economically feasible has been harnessed so far (Department of Electricity Development, 2018).

Hydropower are generally classified as Run-Off-River (ROR), Poundage Run-Off-River (PROR) and Storage hydropower. A dam and a reservoir are used in storage hydropower facilities to impound water, which is then stored and released as needed. Simple strategy behind the storage hydropower is storing water during monsoon season to generate electricity during a dry season. Water stored in reservoirs provides flexibility to generate electricity on demand and reduces dependency on the variability of inflow. Very large reservoirs can store inflow for months or even years, but they are usually designed for seasonal storage, to supply water during dry seasons. Storage hydropower facilities are more flexible than ROR plants, and can be used to produce both base and peak load power due to their ability to shut down and restart at short notice, depending on the power system's demand. Storage reservoirs are frequently developed as multipurpose systems due to their ability to control water flows, giving additional benefits such as flood control, water supply, irrigation, navigation, and recreation. The ability to store significant amounts of energy and

adapt to fluctuating load requirements, from short term (day peaking) to weekly and seasonal variations, is the fundamental advantage of hydropower plants with storage. Such reservoirs are becoming increasingly important and valuable also for storing energy from other renewables, such as wind and solar power. Storage hydropower plant situated in Himalayan or Hilly regions are very likely to have high sediment concentrated water due to fragmentation of chemically composed rock and decomposition of mineral content rock under harsh weather phenomena. One of the most significant obstacles to hydropower development in Nepal is sedimentation. This is due to the fact that the silt load in Nepalese rivers is among the world's largest (Sangroula, 1970). Reservoir sedimentation is a process of erosion, entrainment, transportation, deposition and compaction of sediment carried into reservoirs formed and contained by dams. Sediment is generally a mixture of particles with different sizes as presented in Table 1.1 below (T. R. Bajracharya et al., 2008). Sediment can damage turbines and other mechanical equipment through erosion of the oxide coating on the blades, leading to surface irregularities and more serious material damage. Sustained erosion can lead to extended shutdown time for maintenance or replacement.

Table 1.1: Classification of river sediment

Particle	Clay	Silt	Sand	Gravel	Cobbles	Boulder
Size (mm)	Less than 0.002	0.002-0.06	0.06-2	2-60	60-250	Greater than 250

Many factors determine rates of mechanical abrasion. Of particular importance is sediment type and physical characteristics. Minerals with a Mohs hardness more than 5 – such as quartz, feldspar, and tourmaline – are problematic in angular sediments. Abrasion susceptibility is further affected by hydraulic and facility operation factors such as flow velocity, hydraulic head, turbulence, turbine rotational speed, and turbine material. Impulse turbines, such as Pelton, Turgo etc. are more susceptible to abrasion than are reaction turbines (Review 2010). (Dealing with Sediment: Effects on Dams and Hydropower Generation | Hydro Review, n.d.)

The dynamic movement of silt flowing with water colliding against a solid surface causes sediment erosion. Hydraulic turbine components are subjected to abrasive and

erosive wear when operating in sediment-laden water. This wear not only affects the turbine's efficiency and lifespan, but it also causes challenges with operation and maintenance, resulting in financial losses. This is a worldwide issue with hydropower plant operation and maintenance. Hydraulic turbine components are severely damaged by the high silt concentration paired with the high proportion of quartz in the water. A number of factors can influence the process of sediment erosion damage in hydro turbine components. The erosion intensity depends on the sediment type and its characteristics (shape, size, hardness, concentration etc.), hydraulic design and operating conditions of turbine (flow rate, head, rotational speed, velocity, acceleration, turbulence, impingement angle etc.), and material used for the turbine components. All these factors are needed to be considered for predicting the erosion. Therefore, dealing with sediment erosion problems requires a multidisciplinary approach (Neopane, 2010). Degradation of hydraulic machine especially turbine blades directly depends on sediment (Thapa, 2004).

1.1.1 Kulekhani First Hydropower Station, NEA

Kulekhani First HPS, located at Dhorsing, Makwanpur is the only reservoir type Hydro-electric Power Station in Nepal. It is situated in Lower Mahabharat Range of Makwanpur District, Central region of Nepal at about 30 Km to the Southwest of Kathmandu, whereas the Kulekhani Dam itself is located at about 21 Km Southwest of Kathmandu. It covers two basins of different river systems i.e. the Kulekhani river basin and the upper Rapti river basin neighbouring to south of the Kulekhani river basin. Its installed capacity is 60 MW with two units of 30 MW each. This station was designed as a peaking power station but it is often operated to the system requirements for voltage improvement & system stability.

There are currently twenty hydropower plant under Nepal Electricity Authority of generating capacity categorized as below and above than 30 MW (Nepal Electricity Authority::, n.d.). Except Kulekhani Cascade Hydropower Stations all are Run-Of-River type and are effected heavily by sediment led erosion. Kulekhani First Hydropower Station is a storage hydropower plant feed with faint sediment concentrated water from the Kulekhani reservoir instead it is affected by erosion in gradual manner. KL1HPS has annual siltation rate of 0.65 Mm³ in active volume. Due to high annual siltation the estimated life of reservoir is about 80 years i.e. upto 2100

AD (Shrestha, 2020). Such erosion phenomena is a part of regular monitoring activities for hydropower maintenance. In the present study erosion of bucket due to cavitation has been carried out for Kulekhani First Hydropower Station.

The KL1 hydropower plant generally operated for 4 hour and 3 hour evening and morning peak load respectively due to its ability of handling variable load with great ease. It plays vital role in black start when the national grid system is totally blackout due natural calamities like landslides, heavy strom, flood, heavy rainfall and other technical faults. It takes water from various rivers and tributaries like Sim khola, Chakhel Khola, Palung Khola, Thado khola and Shera Khola along with seasonal tributaries. Inflow are collected during the monsoon season and generate electricity round the year for evening and morning peak load along with fluctuating load demands in national power grid. The water from various rivers and tributaries are collected in huge reservoir with 2.2 km² surface area and about 85.3 * 106 m³ gross storage capacity where the sediments settles down easily to higher extent. Then water through intake gate flows into headrace tunnel and penstock which is about 1353.5 meter in length and 2 to 1.5 varying in diameter and enters into turbine nozzle through control of main inlet valve. The nozzle impinge a jet of water which strikes the bucket of runner coupled with generator to rotate and thus electricity is produced. The water after impacting the bucket falls down to pit and passes through the tunnel for the feed to the Kulekhani Second HPS cascade plant. The salient features of Kulekhani First HPS are as follows:

Table 1.2: Salient features of Kulekhani First HPS

Type	Storage
Location	Dhorsing, Makwanpur
Installed Capacity	60 MW
Rated Head	550 m
Catchments Area	126 km ²
Maximum Discharge	13.1 m ³ /sec
Turbine	
No. and Type	Two, Vertical Shaft Pelton
Installed Capacity	30 x 2 MW
Rated Speed	600 rpm

Generator	
Rated Capacity	35 MVA
Generating Voltage	11kV
Frequency	50 Hz
Dam	Zoned Rock Fill Dam with Inclined Core, 114m high, 406m crest length
Headrace Tunnel	Circular Section, Ø 2.5m x 6,233m in long
Penstock	Ø 2.0-1.5m, 1324m length
Main Transformer	Two, 35 MVA, 11/66 kV

(Brochure of Kulekhani First Hydropower Station, 1982)

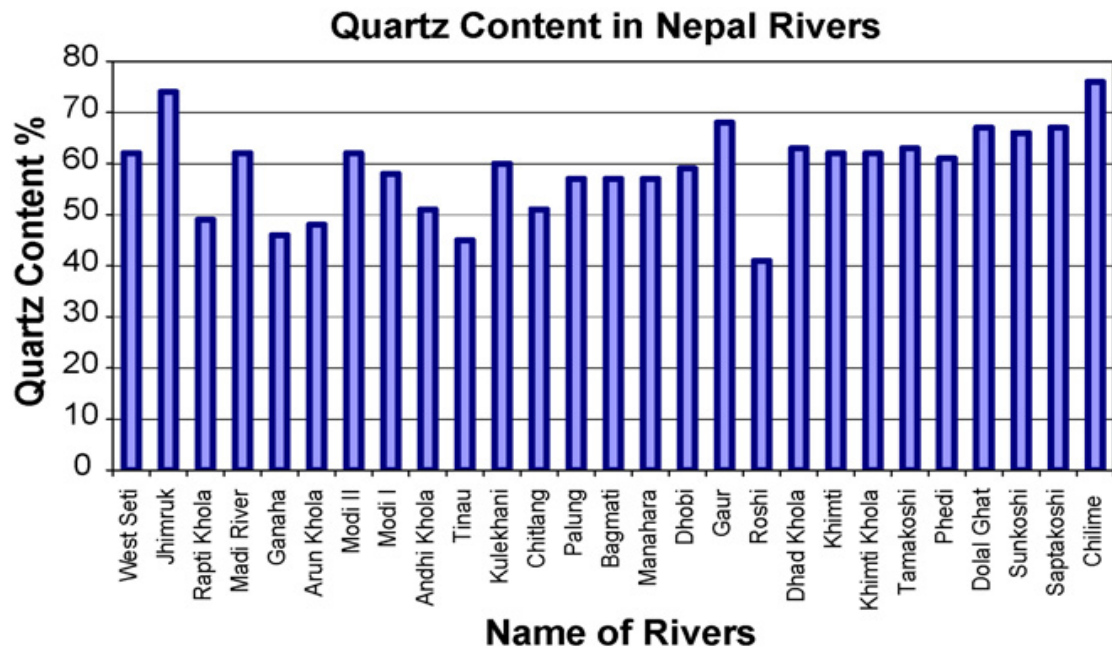


(Source google map 2019)

Figure 1.1: Kulekhani reservoir location

The inflow water for reservoir are mainly from hilly and rocky catchment area. The main sources of sediments are natural decomposition of hard rocks and minerals due to calamity and carried out by rainfall, flood, landslides etc. upto the reservoir. The heavy sediment particle easily settle down in reservoir bed, as per sedimentation survey (Bathymetric survey) sediment deposition layer is increasing day by day thus leading to storage loss, generation loss and reduced reservoir life (Shrestha, 2020). The minute sediment particle which are floating and insoluble flows along with the

water and cause erosion of Pelton runner bucket and nozzles on intermittent operation. The quartz content in the context of Nepalese rivers are as presented below.



(Source: T. R. Bajracharya et al., 2008)

Figure 1.2: Quartz content in Nepalese rivers



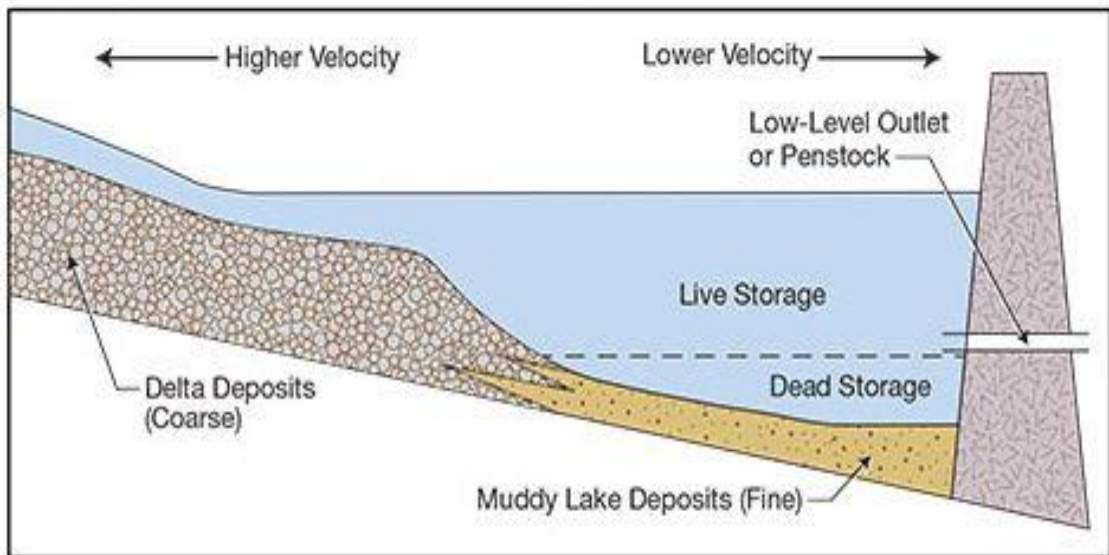
(Source: Site visit 2021)

Figure 1.3: Kulekhani reservoir with sloping intake

1.1.2 Active and dead volume of reservoir

Reservoir volume which can be used for power generation is called active volume or active storage or live storage and the volume which cannot be used for power

generation is called dead volume or dead storage. More is the active volume more will be the power generation capacity of the reservoir. Dead volume is also important because if it is filled completely then power generation will be completely stopped. Sediment may accumulate in active or dead volume region. If the sediment accumulates in active volume region, then the power generation capacity of reservoir plant decreases and if it accumulates in dead volume region, then the life of reservoir decreases.



(Schellenberg, 2019)

Figure 1.4: Active and dead volume of reservoir

1.1.3 Elevation-Reservoir capacity:

The Kulekhani reservoir full of aesthetic view is only one storage reservoir of Nepal planned and constructed for the single purpose of generating electric power to be supplied to the National Grid. The principal features of the reservoir is as follows:

Table 1.3: Kulekhani reservoir features

Features of reservoir	
Catchment area	126 km ²
High water level	EL 1530 m
Low water level	EL 1476 m
Drawdown	54 m
Surface area	2.2 km ²
Gross storage capacity	85.3 × 10 ⁶ m ³

Features of reservoir	
Effective storage capacity	73.3× 10 ⁶ m ³

The storage capacity at each water surface is determined on the basis of equation based on polynomial method as follows:

$$Y = a_0 + a_1 \times (EL) + a_2 \times (EL)^2 + a_3 \times (EL)^3 \quad \text{Equation 1.1}$$

Where, Y: Reservoir storage capacity (10⁻⁶ m³)

EL = Reservoir water elevation (m)

$$a_0 = -226,544.6$$

$$a_1 = 471.98683$$

$$a_2 = -0.3280187$$

$$a_3 = 0.76041656 \times 10^{-4}$$

1.1.4 Reservoir inflow

Inflow are calculated on the basis of daily reservoir parameters as follows:

- RWL₁ at the beginning(m)
- RWL₂ at the end (m)
- Storage at RWL₁ (10³m³)
- Storage at RWL₂ (10³m³)
- Storage increment (4)-(3)/86.4 (m³/S day)

1.1.5 Turbines

Turbines are the vital components among the power generating equipment in hydropower. Turbines are generally categorized into two categories: impulse and reaction type turbine. Impulse type turbine are generally Pelton, Turgo whereas reaction type are Francis and Kaplan. Pelton turbine is an impulse turbine as there is no pressure drop across the buckets. The flow is axial, i.e. there is no change in peripheral velocity and water enters and leaves the buckets at the same radius. The buckets are double hemispherical in shape. The water strikes the bucket in the centre and flows, out at both sides making a U turn. The surface inside the buckets is polished and smooth to reduce hydraulic losses. A costly material like bronze or

stainless steel is generally used for the buckets. The buckets are detachable (Hussian et al., 2008)

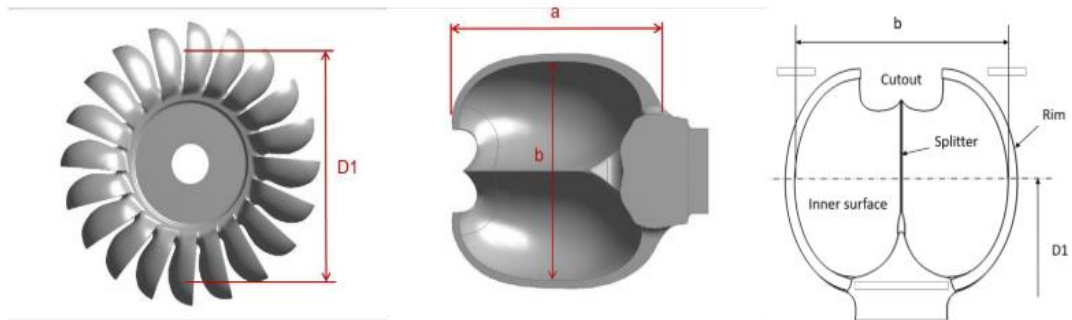


Figure 1.5: Pelton runner bucket

The main dimensions of a Pelton runner bucket are shown above in Figure 1.5. The pitch diameter $D1$ is defined as double the distance between the jet axis and the runner center line, b is the bucket width and a is the bucket height. The main parts of the buckets are the cut out, the splitter and the rim. The cut out is where the jet first enters the bucket, the splitter divides the jet into two streams, and the rim is where the water last interacts with the turbine and is considered the outlet of the bucket. Between the splitter and the rim, the water jet is deflected almost 180 degrees to deliver the maximum available power to the turbine. The Kulekhani Hydropower Station, storage reservoir hydropower plant with head of high range has installed Pelton type turbine. The salient features of Pelton turbine is as follows:

Table 1.4: Feature of turbine of KL1HPS

Features of turbine	
Type	Vertical shaft, Pelton type
Rated output	2 X 31,000 kW
Rated speed	600 rpm (50 Hz)
Gross head	614 m to 560 m
Rated head	550 m
Elevation of runner center	EL. 916
Runner	
Number of buckets	19

Features of turbine	
Width of bucket	490 mm
Pitch circle diameter	1562 mm
Outside diameter	2045 mm
Material	SCS1mod. (JIS G5121)
Weight	3.5 Ton
Nozzle & Neddle	
Number of Nozzle	4
Diameter of Nozzle	190 mm
Design pressure	67.6 kg-f/cm ²
Test pressure	91 kg-f/cm ²
Material	SCW49 (JIS G5102)
Number of Neddle	4
Maximum diameter	235 mm
Material	S25C (JIS G4051)



(Source: Site visit 2021)

Figure 1.6: Pelton runner of KL1HPS

1.1.6 Plant efficiency

Efficiency is simply the ratio of output to input. Plant efficiency is the essential parameter of hydropower station to be considered while generating power. Turbine efficiency plays vital role in maintaining plant efficiency (Poudel et al., 1970). The impact of erosion on runner bucket due to cavitation is easily noticeable through the fluctuations of efficiency. Higher the erosion on runner bucket lower will be the generating efficiency. The plant efficiency or overall efficiency depends upon mechanical and hydraulic efficiencies. The simple equation of efficiency was used to determine the respective efficiency while generating power associated with effective head and reservoir water level. The general equation for efficiency is as follow:

$$\eta = P / (\rho \times g \times Q \times H) \quad \text{Equation 1.2}$$

Where, η is efficiency

P = Power (Watt)

ρ = Density of water (kg/m^3)

Q = Discharge (m^3/s)

H = Effective head (m)

1.2 Problem statement

Hydropower plants are generally uninterrupted operations in nature. Faults and break down occurs very often. So various types of maintenance work like general repair to overhauling are required as per nature of fault and incur huge budget as well. Maintenance is considered as the back bone of hydropower plants. Planned maintenance plays vital role in efficient as well as economic operation of hydropower plants. It also minimizes the down times and avoid emergency Break-Down to higher extent. Budgeting & Scheduling for planned maintenance is wise decision in hydropower plants as its operation is interruptible and economically very sensitive. Predicting the wear and tear of generating equipment like Runner, Buckets and Nozzles are very challenging. In the case of Kulekhani First HPS, a storage hydropower plant on long run some erosion observed on bucket and injector. As the sediment concentration of storage hydropower plant is very low, it could be understood that the major contribution to erosion on long run is due to cavitation. In this study, erosion of Pelton turbine on due to cavitation is proposed for study. With long run operation, by analysing water consumption trend of generating units, efficiency deterioration will be studied. Photographic observations of turbine on different operating time shall give the idea about cavitation prone areas. Comparison with literatures (of CFD modelling of runner) shall finally give idea about erosion of Pelton runner due to cavitation phenomena and sand particle led erosion, which would provide insights for scheduling and budgeting for planned maintenance in Pelton turbine operated hydropower plant.

1.3 Objectives

The main objective of the research is to study about efficiency deterioration of Pelton turbine in long run due to cavitation led erosion.

Specific objectives are

- To analyse water consumption trend of the Pelton turbine generating units on long run and identify efficiency deterioration.
- To analyse wear rate of Pelton turbine and identify contribution of cavitation.
- To perform 2-D computational fluid dynamics (CFD) modelling of the Pelton turbine system for cavitation modelling.

1.4 Assumptions and limitations

- Dry season data are considered for analyzing water consumption trend.
- Full load condition i.e. 60 MW is considered.
- Effect of cavitation is similar for all the buckets. Hence only, a single bucket is considered for analysis.
- Water temperature is constant.
- For calculating water consumption trend of generating units, losses due to evaporation and seepage are not considered.

CHAPTER TWO: LITERATURE REVIEW

Different relevant literatures related to erosion of Pelton turbine has been reviewed. The different journal papers, previous works done on the same field by different concerned organization gives clear idea about the past researches done on the field of sand and silt abrasion erosion of Pelton turbine. But few research works are carried out on erosion due to cavitation on Pelton runner and are also controversial. The research that should be done was identified.

2.1 Theory of Pelton Turbine

Pelton turbine is a type of tangential flow impulse turbine used in hydroelectric power plants to generate energy. L.A. Pelton, an American engineer, discovered this turbine. The only energy available at the Pelton turbine's input is kinetic energy. For the high head, this type of turbine is used. The nozzle converts the entire potential energy of the high head water to a form of high speed jet. As the turbine is set at atmosphere, atmospheric pressure is present at the turbine's input and exit.

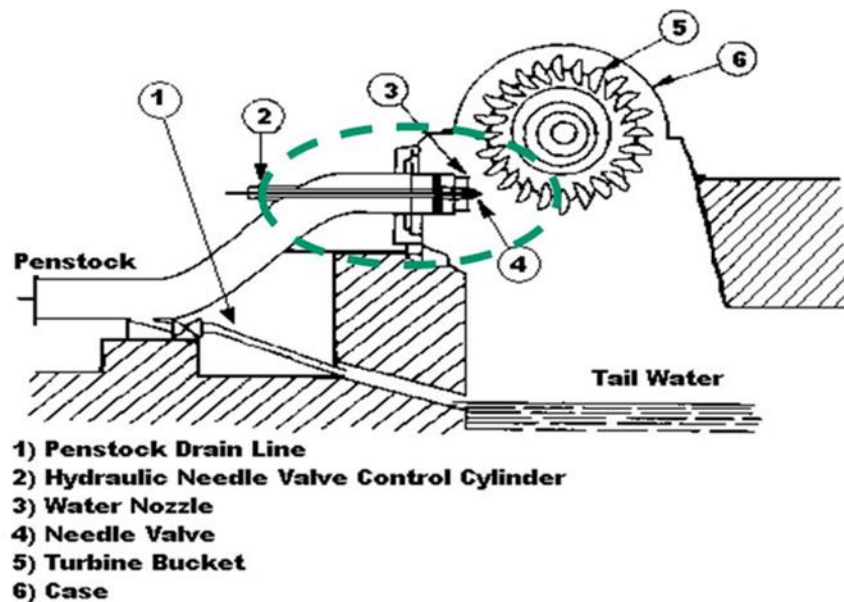


Figure 2.1: Parts of a Pelton Turbine

Power demand may fluctuate over time. This criterion is met by a controlling mechanism that governs the position of the spear head. The spear tip, part number 3 in figure 2.1 at the water inlet nozzle is moved in as the power requirement decreases. As a result, the rate of water flow is reduced. If the demand for power rises, the spear head will be moved out, increasing the flow rate.

The bucket is the most important part of a Pelton wheel. To avoid fatigue failure, buckets are cast as a single solid piece. The force pushing on the turbine bucket does not remain constant throughout time. If we follow one bucket, we will notice that it has a strong force for a short time (during the time of jet impingement), then a longer idle period with no jet interaction. As a result, the force pushing on the bucket isn't consistent. It fluctuates with the passage of time, yet it is cyclic in nature. Such cyclic force will readily lead to premature fatigue failure if buckets are manufactured with welding connection components. A splitter is used to divide a water jet into two equal components. The jet turns nearly 180 degrees due to the bucket's unique form. An impulsive force is created on the bucket as a result of this. Newton's 2nd law of motion can be used to calculate the force produced. In order to enhance impulsive force, blade outlet angles of 180 degrees are commonly used. On the bottom half of the buckets, a cut is made. This ensures that the water jet from nozzle will not get interrupted by other buckets due course of rotation.

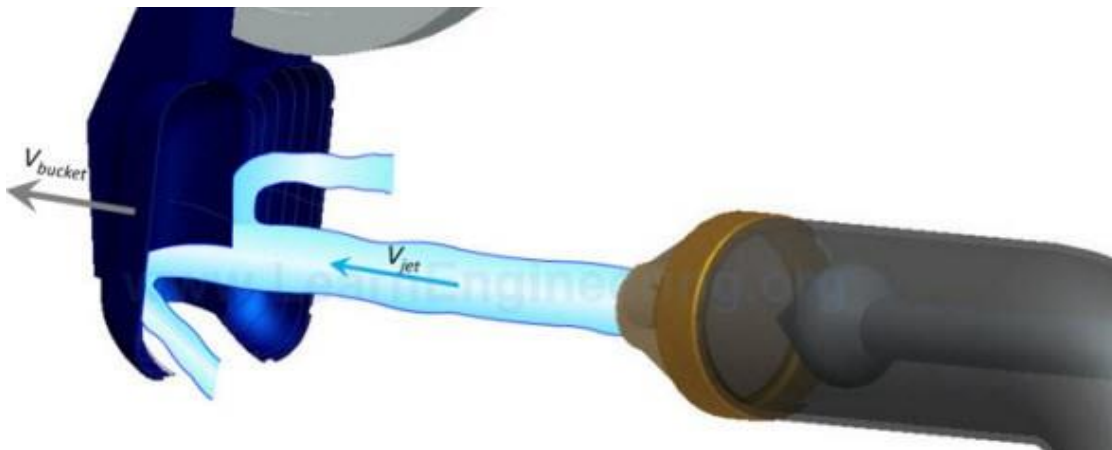
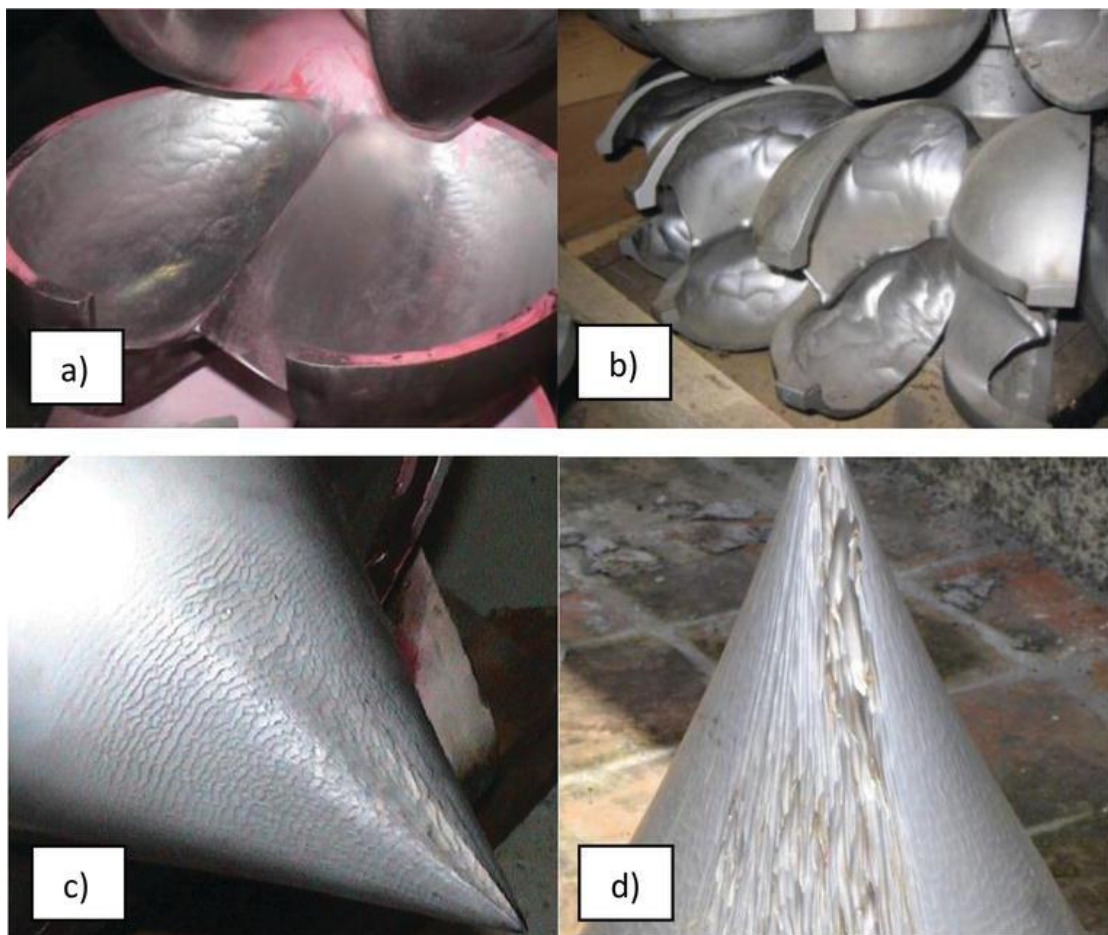


Figure 2.2: Working of the Pelton turbine

2.2 Erosion in turbine

Erosion in a turbine is a phenomena of gradual removal of molecule from the metallic surface. The solid particle that causes the removal of parent material is called sediments. In the case of turbine sediment erosion is a phenomena of mechanical wear due to the dynamic action of sediment flowing along with water impacting against a solid surface of hydraulic components (Neopane, 2010). Generally solid particle flowing with the water are harder than the parent material of turbine. Generally material removal in hydraulic machinery are mainly due to erosion, cavitation pitting and corrosion. Under range of high head operation Pelton and Francis turbine are often affected by sand erosion. The efficiency of eroded turbine decreases and poses a

weak structure (Thapa, 2004). In the case of Pelton turbine, all the hydraulic energy of water is converted into kinetic energy before runner inlet. In Pelton turbine usually the jet velocity is usually higher than 100 m/s. As commonly understood, velocity is of the determining variable for solid particle erosion, the rise in velocity make the flow more turbulent, increasing the erosion rate. Literatures classify the erosion of Pelton turbine into four parts for research purpose first inlet and valve, second the nozzles, third the runner and finally the casing. Out of these components, nozzle system and runner are mostly vulnerable to erosion. In the nozzle, a strong turbulent effect occurs on the needle surface due to very high velocity at the nozzle outlet and the needle surface.



(Neopane et al., 2011)

Figure 2.3: Eroded Pelton turbine components

While most of the literatures are focused on sand particle led erosion of Pelton turbine and systems, only a few authors have written about the cavitation in Pelton turbine nozzle and bucket.

2.3 Cavitation phenomena

Simply cavitation is defined as the natural phenomena of the formation, growth and collapse of vapour filled cavities or bubbles in the flowing liquid due to local fall in fluid pressure. It is well known that when velocity of flow increases, the pressure falls. In liquids the pressure cannot fall below vapour pressure which depends upon the temperature and height above mean sea level of the site. If the pressure drops below the evaporation pressure the liquid boils and a large number of small bubbles of vapour are formed. These low-pressure bubbles are carried by the stream to higher-pressure zones, where the vapour condenses and the bubble collapses abruptly. As a result, a cavity forms, and the surrounding liquid rushes to fill it. Streams of liquid from all directions smash at the cavity's center, creating a very high local pressure. The process of cavity formation and high pressure is repeated hundreds of times per second. When a liquid is heated to its boiling point, it converts into a vapour, which is known as boiling. When the vapour pressure of a liquid equals the atmospheric pressure exerted on the liquid, the liquid transitions to a gaseous phase. . Figure below shows the variation of boiling point of water with the saturation pressure. By saturation pressure, we should understand that it is the pressure for a particular temperature at which the liquid starts to evaporate or boil. Figure 2.4 shows the variation of boiling point of water with saturation pressure. With decreasing pressure there is decrease in the boiling point of water.

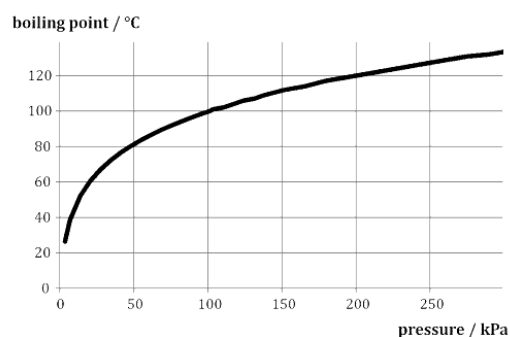


Figure 2.4: Saturation pressure against temperature (of Water)

Due course of flow, there are certain regions in flow regime at where the pressure is sufficiently low and in such area the liquid boils forming a bubble cavity. This bubble then transfers along with the flow to a high pressure region where it collapses forming

a micro-jets (local pressure upto 4000 bar) which impinges upon the solid surface causing small amount of material to erode.

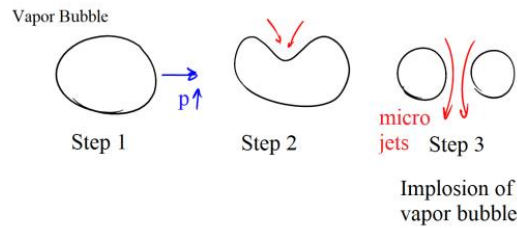


Figure 2.5: Phenomenon of cavitation

Theoretically,

For a nozzle, applying energy conservation equation (the Bernoulli equation),

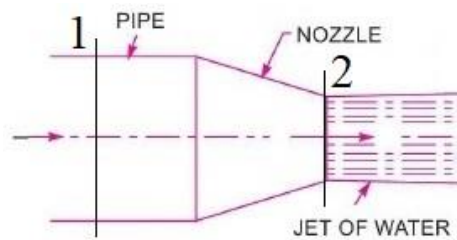


Figure 2.6: Water jet

For figure 2.6, applying the Bernoulli equation at section 1 and 2

$$p_1 + \frac{1}{2}\rho v_1^2 = p_2 + \frac{1}{2}\rho v_2^2 \text{ Equation 2.1}$$

From the equation it follows that speed increase leads to local pressure decline (proportional to squared speed value). As we move downstream of the nozzle, at point 2 the nozzle converts entire pressure energy of the water to kinetic energy in form of a high speed jet. As it follows from equation, in the flow (Figure 2.6), the water accelerates and undergoes decrease of local pressure. If the pressure falls to the level of saturated vapour pressure, cavitation is formed.

Cavitation is mathematically represented by dimensionless criteria σ , also called cavitation factor, and further specified by the equation:

$$\sigma = \frac{p_r - p_{sat}}{\frac{1}{2}\rho v_r^2} \text{ Equation 2.2}$$

Where,

σ = Cavitation Number

p_r = Reference pressure

p_{sat} = Vapour pressure of liquid for given temperature

ρ = Density of liquid

v_r = velocity of the liquid

Cavitation number can be used as an indicator of the likelihood of cavitation. Since cavitation number reduces with increasing velocity, it should be kept in mind to prevent abrupt increase in velocity to a high numeric value.

2.4 Computational Fluid Dynamics

Computational Fluid Dynamics (CFD) is a field that employs computer resources to simulate flow issues. To simulate a flow problem, problems are solved using mathematical, physical, and programming methods, after which data must be generated and analyzed. Partial differential equations govern fluid (gas and liquid) flows, which represent mass, momentum, and energy conservation laws. Computational Fluid Dynamics (CFD) is the art of replacing such PDE systems by a set of algebraic equations which can be solved using digital computers. Computational Fluid Dynamics (CFD) provides a qualitative (and sometimes even quantitative) prediction of fluid flows by means of fluid flow by means of

- Mathematical modeling (partial differential equations)
- Numerical methods (discretization and solution techniques)
- Software tools (solvers, pre- and post-processing utilities)

In order to provide easy access to their solving power all commercial CFD packages include sophisticated user interfaces to input problem parameters and to examine the results. Hence all codes contain three main elements: (I) a pre-processor, (II) a solver and (III) a post processor. We briefly examine the function of each of these elements within the context of a CFD code.

ANSYS CFX and ANSYS Fluent are the commercial CFD codes available. The main difference between these is the way solvers integrate the flow equations and solution strategies. CFX uses finite volume elements to discretize the domain. Contrarily, Fluent utilizes finite volumes. They are both control volume based solvers, which ensures conservation of flow quantities. The CFD analysis of Pelton turbine in the paper is carried out using ANSYS CFX.

2.4.1 Pre-Processor

Pre-processing consists of the input of a flow problem to a CFD program by means of an operator-friendly interface and the subsequent transformation of this input into a form suitable for use by the solver. The user activities at the pre-processing stage involve:

- Definition of the geometry of the region of interest: the computational domain.
- Grid generation-the sub-division of the domain into a number of smaller, non-overlapping sub-domains: a grid (or mesh) of cells (or control volumes or elements).
- Selection of the physical and chemical phenomena that need to be modelled.
- Definition of Fluid properties.
- Specification of the appropriate boundary conditions at cells which coincide with or touch the domain boundary.

2.4.2 Solver

There are three distinct streams of numerical solution techniques: finite difference, finite element and spectral methods. In outline the numerical methods that form the basis of the solver perform the following steps:

- Approximation of the unknown flow variables by means of simple functions.
- Discretization by substituting of the approximations into the governing flow equations and subsequent mathematical manipulations.
- Solution of the algebraic equations

The main differences between the three separate streams are associated with the way in which the flow variables are approximated and with the discretization processes. Here we have employed finite volume method.

2.4.3 Post-Processor

Owing to the increased popularity of engineering workstations, many of which have outstanding graphics capabilities, the leading CFD packages are now equipped with versatile data visualization tools. Some of them are

- Vector Plots
- Surface Plots

- Particle Tracking

2.5 The finite volume method

The finite volume method was originally developed as a special finite difference formulation. The Numerical algorithm consists of following steps:

- Formal integration of the governing equation of fluid flow (Continuity and Navier-Stokes Equation) over all the control volumes of the solution domain.
- Discretization involves the substitution of a variety of finite difference type approximations for the terms in the integrated equation representing flow processes such as convection, diffusion and sources. This converts the integral equations into a system of algebraic equations.
- Solution of the algebraic equations by an iterative method.

2.5.1 Continuity and Navier-Stokes Equation

The continuity and Navier-Stokes equation in cylindrical coordinates are described below:

$$\frac{\partial V_r}{\partial r} + \frac{\partial V_z}{\partial z} + \frac{V_r}{r} = 0 \quad \text{Equation 2.3}$$

$$V_r \frac{\partial V_\theta}{\partial r} + V_z \frac{\partial V_\theta}{\partial z} - \frac{V_r V_\theta}{r} = \nu \left(\frac{\partial^2 V_\theta}{\partial r^2} + \frac{\partial V_\theta}{r \partial r} - \frac{V_\theta}{r^2} + \frac{\partial^2 V_\theta}{\partial z^2} \right) \text{Equation 2.4}$$

$$V_r \frac{\partial V_r}{\partial r} + V_z \frac{\partial V_r}{\partial z} - \frac{V_\theta^2}{r} + \frac{\partial \rho}{\rho \partial r} = \nu \left(\frac{\partial^2 V_r}{\partial r^2} + \frac{\partial V_r}{r \partial r} - \frac{V_r}{r^2} + \frac{\partial^2 V_r}{\partial z^2} \right) \text{Equation 2.5}$$

$$V_r \frac{\partial V_z}{\partial r} + V_z \frac{\partial V_z}{\partial z} + \frac{\partial \rho}{\rho \partial z} = g + \nu \left(\frac{\partial^2 V_z}{\partial r^2} + \frac{\partial V_z}{r \partial r} + \frac{\partial^2 V_z}{\partial z^2} \right) \text{Equation 2.6}$$

Where, V_θ , V_r and V_z are tangential, radial and axial velocity components respectively, ρ is fluid density, g is gravitational acceleration and ν is kinematic viscosity. Due to the complexity of the equations, it's extremely difficult to get an analytical solution directly. (Robert W Fox, 2010)

2.5.2 Turbulence Modelling

Turbulence modelling is the construction and use of a model to predict the effects of turbulence. A turbulent fluid flow has features on many different length scales, which all interact with each other. A common approach is to average the governing equations of the flow, in order to focus on large-scale and non-fluctuating features of the flow. However, the effects of the small scales and fluctuating parts must be

modelled (Versteeg & Malalasekera, 1995). In this study, based on literatures RNG k-epsilon model is used for it has shown better results in rotating cavities.

2.6 Past research done on erosion of Pelton turbine

In former research “Numerical analyses of cavitating flow in a Pelton turbine” the author applied CFD model for the study of cavitation mechanism in Pelton turbine and concluded that Pelton runner are affected by pitting cavitation. As per author analysis different evaporation mechanics occurs when the bucket moved into the jet. Despite this, the jet is surrounded by air at ambient pressure, dynamic effects and the high unsteadiness during the cut-in caused the absolute pressure to drop below the water vapor pressure (Rossetti et al., 2014).

Another research work under “Study of combined effect of sand erosion and cavitation in hydraulic turbines” revealed that a perfect hydraulic design component should be cavitation-free as per principle. But changes in surface integrity due to sand erosion even a cavitation-free design are found prone to cavitation. Rotating Disc Apparatus (RDA) was used as test set up by author for research work and concluded that there is a possibility of combined effect of sand and cavitation in the hydraulic turbine components. Surface roughness due to sand erosion at high velocity region may initiate cavitation erosion. The synergic effect of sand and cavitation is more penetrating than their individual effects (Thapa et al., 2007).

Similar research on “Numerical simulation of cavitation flow characteristic on Pelton turbine bucket surface” in order to investigate cavitation phenomena suitable numerical model and method for simulation of cavitation on Pelton bucket surface were run and concluded that predicted cavitation area is in good accordance with the low pressure area in the two phase simulation. Also cavity would initial near the cut-out on the front surface at the beginning phase of bucket cutting through the free jet hence decrease the output of Pelton runner (Zeng et al., 2015)

A paper presented on “Detailed analysis of flow in two Pelton turbines with efficiency and cavitation prediction” on the basis of numerical analysis for cavitation prediction put forward that small vapour cavity at the inner side and a larger one at the back side of the bucket were observed but their condensation process was very slow thus resulting that conditions for cavitation pitting are not fulfilled and no cavitation damages should be expected (Jošt et al., 2019).

The past research work has been done on “Sand Erosion of Pelton turbine nozzles and buckets: A case study of Chilime Hydropower “The researchers has collected the sample of sand and water from Chilime river and conducted an experiment. The researchers found out asfollowing wear rate relation of Pelton turbine buckets and found that erosion rate is 3.4 mm/ year, turbine efficiency is reduced by 1.21 % and as a consequence loss in the power generation. (T. R. Bajracharya et al., 2008).

Erosive wear rate $\propto a (\text{size})^b$

Where; erosive wear rate is in mm/year, and

$a = 351.35$ and $b = 1.4976$, for quartz content of 38%

$a = 1199.8$ and $b = 1.8025$, for quartz content of 60%;

$a = 1482.1$ and $b = 1.8125$, for quartz content of 80%;

Relationship between erosion rate and the reduction in efficiency was expressed as;

Efficiency reduction $\propto a (\text{erosion rate})^b$

Where $a = 0.1522$ and $b = 1.6946$

Similarly, various researchers have conducted experiments to study the effect of parameters such as: size, hardness and concentration of silt particles, velocity of flow, properties of the base material of the turbine components and operating hours of the turbine on erosive wear and found out that erosive wear rate increases with an increase in the silt concentration irrespective of the silt size. However, for a given value of silt concentration, the erosion rate has been found to be higher for larger size particles as larger particles have higher impact energy. Using experimental data a correlation for erosive wear rate was developed as a function of particle size, silt concentration, jet velocity and the time of operation which has been found to have a good agreement with experimental data of test rigs.(Padhy & Saini, 2009)

Correlation for normalized erosive wear rate is obtained as follows:

$$W = 4.02 \times 10^{-12} (S)^{0.0567} (C)^{1.2267} (V)^{3.79} (t)$$

Where

S = Silt size

C = Silt concentration

V = Water Jet Velocity

t = Operating hours of the turbine

Senapati et al. on their research paper explores the quantification of metal loss due to silt erosion under laboratory condition. Mild steel test specimen set at angles of 50, 450 and 900 in the slurry flow direction were exposed to silt attack in a pot test rig in the laboratory. The total period of exposure of the specimen to the silt attack was maintained for four hours, at steps of one-hour interval each. SiO_2 particles in the size range of 90-250 μm were embedded in tap water to constitute the slurry. The slurry concentration was maintained at 7500 ppm. The shaft carrying the test specimen was rotated at 4032rpm in the slurry to maintain an equivalent water head of 89.85metres. The surface hardness of the specimen increased progressively with the increase in the time of exposure. Maximum Average metal loss was recorded for the sample inclined at 450 in the direction of silt flow while it was minimum for the 900 samples. The experimental results were in good agreement with the theoretical calculated value for metal loss obtained using Finnie's model. (Senapati et al., 2017)

The Phd thesis research work on Sediment erosion on hydro- turbine done by Hari Prasad Neupane revealed that predicted erosion rate density is in good agreement with the experiments. It has been found that erosion process is strongly depended on the shape of the particle. Furthermore, the significant reduction of erosion rate can be achieved by operating turbine in best efficiency point as far as possible. (Neupane, 2010)

Similarly, the research works done on the classification and field study of hydro-abrasive erosion in Pelton buckets. In this study, the hydro-abrasive erosion is classified and measurement methodology is proposed for various erosion patterns in Pelton buckets. In Pelton buckets of a high head hydropower plant located in the Himalayas in India, the amount, pattern and depth of erosion were measured during the study period May-October, 2015. The size, shape and concentration of the suspended sediment passing through the turbines were obtained from manual samples and with an online multi-frequency acoustic instrument. In uncoated buckets, the average reduction of the splitter height and the abrasion in the cut-out portion were 3% and 5% of the bucket width respectively, whereas the maximum erosion depth of ripples in the curved zone was 1.5%. 73% of suspended sediment consisted of silt

particles with median grain size (d_{50}) between 20 and 40 μm . With coefficient of variation 75%, 32% and 1% for concentration, d_{50} and shape respectively, 12,540 t of suspended sediment passed through each turbine unit during 3180 h of operation. This study seeks to facilitate the measurement of hydro-abrasive erosion in Pelton turbines and suspended sediment parameters.(Rai et al., 2017)

A literature survey on abrasive wear in hydraulic machinery considers the factors affecting abrasive wear-the properties of the solid particles, the construction materials and the flow-and various types of wear and concluded the following findings as follows:

1. Wear \propto (Velocity)ⁿ
2. Wear increases rapidly when the particle hardness exceeds that of the metal surface being abraded.
3. Wear increases generally with grain size, sharpness and solids concentration. Rubber lining is particularly vulnerable to large, sharp particles.
4. Wear increases rapidly with flow velocity, and is often reported as being approx. y_c (velocity)³, or cc (pump head) ^{3/2} from both theoretical considerations and test results. (Truscott, 1972)

As per International Electro technical Commission (IEC 62364 Hydraulic machines – Guide for dealing with hydro-abrasive erosion in Kaplan, Francis, and Pelton turbines) the particle abrasion rate in the turbine, the following formula is considered(ISO 14026, 2014):

$dS/dt = f(\text{particle velocity, particle concentration, particle physical properties, flow pattern, turbine material properties, other factors})$

However, this formula being of little practical use, several simplifications are introduced. The first simplification is to consider the several variables as independent as follows:

$dS/dt = f(\text{particle velocity}) \times f(\text{particle concentration}) \times f(\text{particle physical properties, turbine material properties}) \times f(\text{particle physical properties}) \times f(\text{flow pattern}) \times f(\text{turbine material properties}) \times f(\text{other factors})$

The next simplification consists in assigning values to the functions. In the following equations the numerical values for the parameters, without units, have to be used. The units in which the values should be based are given below:

$f(\text{particle velocity}) = (\text{particle velocity})^n$. In the literature abrasion is often considered proportional to the velocity raised to an exponent, n . Most references give values of n between 2 and 4. In this guide we suggest to use $n = 3,4$. Particle velocity in m/s,

$f(\text{particle concentration}) = \text{particle concentration in kg/m}^3$,

$f(\text{particle physical properties, turbine material properties}) = K_{\text{hardness}} = \text{function of how hard the particles are in relation to the material at the surface. At the present stage we suggest to use } K_{\text{hardness}} = \text{fraction of particles harder than the material at the surface,}$

$f(\text{flow pattern}) = K_f / RSp$ ($K_f = \text{constant for each turbine component, } RS = \text{turbine reference size in m, } p = \text{exponent for each turbine component}$). K_f considers impingement angle and flow turbulence. RSp considers part curvature radius,

$f(\text{particle physical properties}) = f(\text{particle size, particle shape, particle hardness}) = f(\text{particle size}) \times f(\text{particle shape}) = K_{\text{size}} \times K_{\text{shape}}$. Note that in this simplification it is assumed that there is no influence from the particle hardness for this function. The particle hardness is considered in the K_{hardness} factor,

$K_{\text{size}} = \text{median diameter of particles in mm,}$

$K_{\text{shape}} = f(\text{particle angularity})$. It is believed that K_{shape} will increase with the degree of irregularity of the particles. Specific data is not available at present but several literature references indicate that K_{shape} varies from 1 to 2 from round to sharp,

$f(\text{turbine material properties}) = K_m$. In this guide we consider $K_m = 1$ for martensitic, stainless steel with 13 % Cr and 4 % Ni and $K_m = 2$ for carbon steel. For coated components K_m should be smaller than 1,

$f(\text{other factors}) = 1$.

So the final, time integrated formula becomes: $S = W^{3,4} \times PL \times K_m \times K_f / RSp$

S is the numerical value of the abrasion depth in mm.

The simplest of the various erosion criteria employs the factor $H \times C$, where H is the net head of the turbine in meters and C is the average annual particle concentration in g/l of all particles with a diameter of $> 50 \mu\text{m}$ (Gummer, 2018). The proposed ranges for hydro-abrasive erosion damage risk are:

$H \times C = > 7$: severe;

$H \times C = >0.7$ and < 7 : moderate; and

$H \times C = < 0.7$: negligible.

The modified particle concentration factor, proposed by Nozaki as an extension of the Zu Yan technique, is the product of the annual average particle concentration in g/l with modifying coefficients related to particle size, hardness, shape, and runner material. $PE = P \times a \times k_1 \times k_2 \times k_3$

Where:

- PE is the modified suspended concentration in g/l;
- P is the measured suspended concentration in g/l; and
- Factors a , k_1 , k_2 , and k_3 depend on the type and geometry of the particles and type of runner material

Also by Krause and Grein proposed the abrasion rate on conventional steel Pelton runner made of X5CrNi 13/4 which was expressed by the expression given below;

$$\delta = PQCV^{3.4} f(D_{50})$$

Where δ is the erosive wear rate (mm/h); P is a constant, Q is the quartz content, C is the mean concentration, V is the relative jet velocity and $f(D_{50})$ is a function defining particle size.

Most of the authors have concentrated their study on sand particle led erosion of Pelton turbine and systems and only few have investigated about the cavitation in Pelton turbine. With sand content analysis of Kulekhani first hydropower station, it was seen that the sediment present in water has very less potential to erode the turbine parts, but on the long run, pitting of bucket was observed. Hence, it was thought that investigation about the causes and effects of efficiency deterioration of Pelton turbine units at KL1HPS is of great significance.

CHAPTER THREE: RESEARCH METHODOLOGY

Research methodology performed under this study are commonly followed steps in such type of research. The consecutive steps are problem identification, literature review, case study, data collection, modelling, analysis, evaluation, and findings, conclusion and recommendation. Under problem identification as first step was to sort out the problems regarding the erosion due to cavitation of Pelton turbine. As area of study was sorted out so various relevant research work and filed study were done like journal papers, conference papers, and power house visit. A case study of Kulekhani First Hydropower Station was considered for this study. The research methodology consecutive steps are presented in flow chart below:

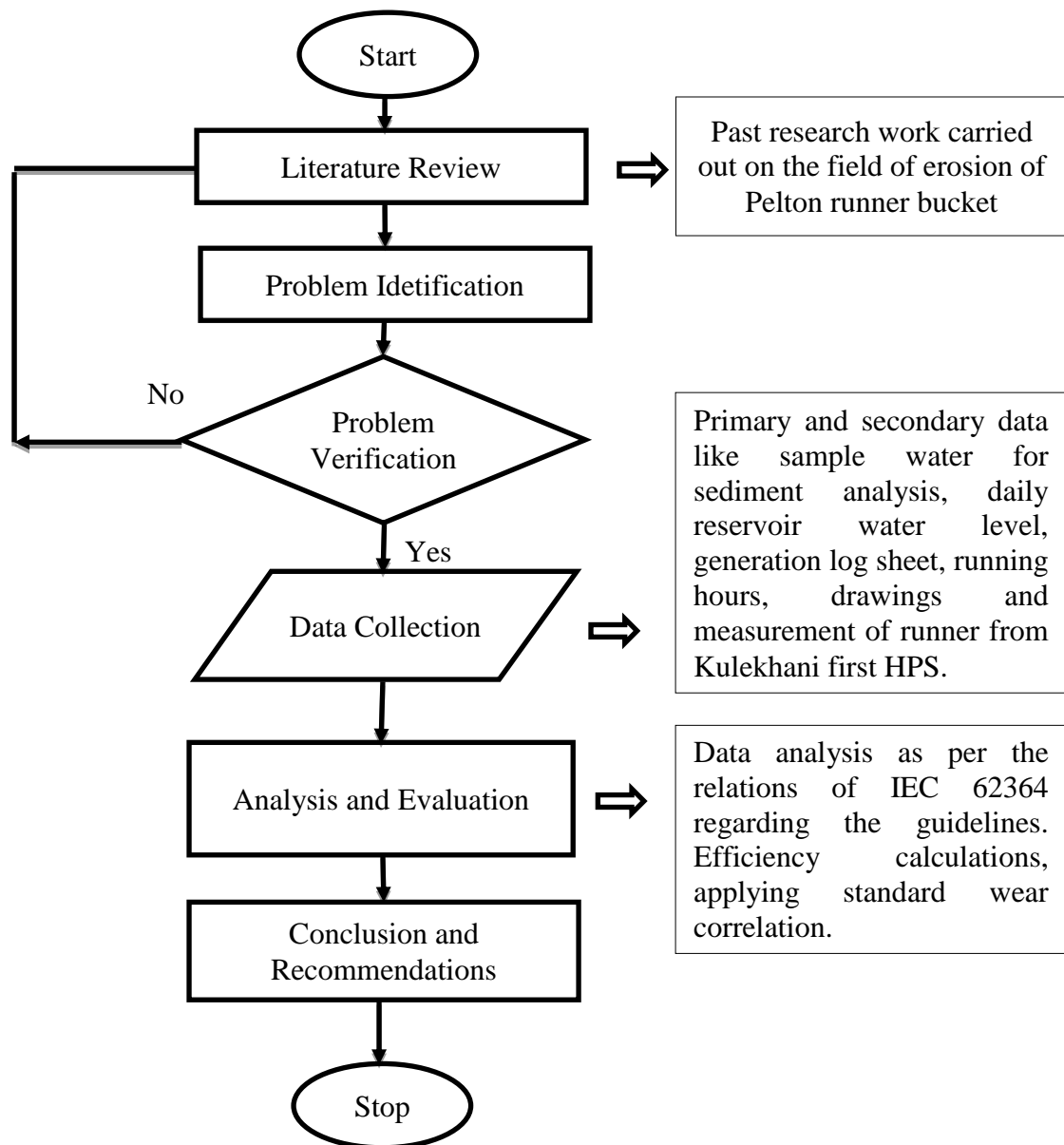


Figure 3.1: Research methodology chart

3.1 Literature Review

Reviewing the articles and journal papers provide insights to the degree up to which any works or researches or studies are put forth by the scholars from the past to the present. Pelton turbine working principle, material compositions, the different theories regarding wear & tear along with remedies and models required for giving right track to this thesis work are to be studied first. The advancement on the past turbine designs, the implementation of the new turbine technologies and their limitations, the methodologies used in the previous studies, the way of setting up laboratory and test rigs for performing experiments are necessary to be understood briefly before proceeding to the next stage.

3.2 Data Collection

The primary and secondary data has been collected from various sources of Kulekhani First Hydropower Station, reservoir and its dam area during site visit. The relevant data for this thesis were extracted into soft copy from the collected raw data like hard copy of daily log sheets, historical photographs, charts, physical measurements and sample etc as described below.

- The sample (5 No.) of reservoir water feeding to turbine was collected in poly-bottle provided by sediment test laboratory from site as per guideline of International Electro-Technical Commission (IEC 62364) and transferred to laboratory for sediment analysis test (ISO 14026, 2014).
- Under laboratory various relevant test like sediment concentration (ppm) analysis, mineral content analysis, particle size distribution analysis, shape and sizes analysis of sediments were conducted. The result were collected from the laboratory.
- Kulekhani First Hydropower Station was visited to collect the various relevant data like log sheets of daily generation, daily reservoir water level, daily running hour, turbine old photograph from their collections and new photograph were also clicked during visit.
- Questionnaires with the Station Chief, Engineer and Operators regarding the regular operations, maintenance practices and nature of erosion of turbine.

- The eroded runner bucket of unit-1 installed was selected for wear and surface texture measurement using proper tools like Profile-gauge and Filler gauge as per instruction of Fuji Electric Co. mentioned in manual under instruction and guidance of technical team of KL1HPS.
- Numerical values were fed in mathematical standard relation to determine reservoir level associated inflow volume of water, effective head, efficiency and wear etc.
- On the basis of thorough observation, rigorous measurement and analysis, fruitful conclusion were drawn.

3.3 Sediment concentration

The sample water collected from site of KL1 HPS were brought to laboratory. Sediment Concentration Analysis was carried out at laboratory. Weighing the original water sample, then carrying out the filtration; followed by drying and again weighing dry sample and hence calculating the ppm were the procedures which was followed by laboratory technicians. Standard filtration method was adopted for sediment concentration analysis. The filtration paper used for the analysis was of 11-micron capacity.

Table 3.1: Sediment concentration of Kulekhani First HPS feed water.

Measurement No	Date	Time	Sediment Concentration (ppm)	Remarks
0	2078/03/21	11:00	48	Only Unit-1 running
1+4	2078/04/05	2:00	70	Unit-1 & Unit-2 running
2	2078/04/06	11:00	292	Both Unit Shut-Down
3	2078/04/06	3:00	68	Only Unit-2 running

3.4 Mineral Content

The samples were transported to Kathmandu and mineral Content Analysis was conducted using zoom stereo type microscope by manual observation method. Each sample was divided into four sets and analyzed separately and then average of the

individual readings was calculated to identify the mineral content of that sample. Hence, 88.5 percent of the mineral grains in the sediment contains minerals with hardness greater than 5 in Mohs' hardness scale which are Quartz, Feldspar, Tourmaline (1.8%), Hornblende (0.6%) and other hard minerals/rock fragments (~1.4%) as shown in Table 5. Hence, they can abrade the turbine material. Remaining 11.5 percent of material comprises Mica (7.8%), calcite (0.9%), clay lumps, highly weathered rock fragments, etc. which possess hardness lower than 5 in Mohs' scale.

Table 3.2: Mineral content in Kulekhani First HPS feed water

Mineral	Percentage of various mineral grains (%)				Mohs' Hardness	
	Observation 1	Observation 2	Observation 3	Observation 4		
Quartz	64	60	71	57	7	
Feldspar	20	29	16	21	6	
Mica	8	5	4	14	2.5 - 3	
Other	A	6	3	5	2	≥5
	B	2	3	4	6	<5

Note:

Other A: Tourmaline, Hornblende, and other hard rock fragments

Other B: Calcite, clay lumps, highly weathered soft rock fragments, and few unidentified sediments.

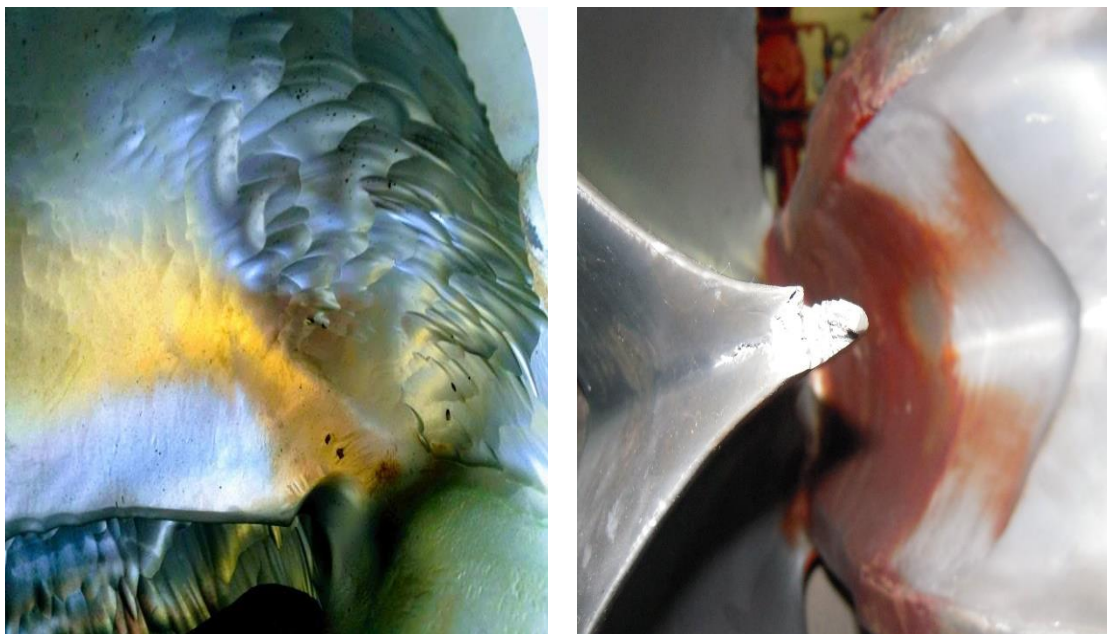
3.5 Particle size distribution

The samples collected from the site were transported to the laboratory and carried out PSD test by laser diffraction method using Beckman Coulter Particle Size Analysers of capacity range of 0.4 micron to 2,000 microns. Laser diffraction method uses the scattering pattern of laser beam to determine the particle size of the sediment samples. The standard procedure provided by the equipment manufacturer was adopted for conducting the PSD analysis. The PSD analysis result of data (sample dated 21 July) is in range of 0.001 to 1 mm.

3.6 Technical observations

In order to have proper observation Kulekhani First Hydropower Station was visited. Actual dimensional drawing and photographs of Pelton turbine clicked during

overhauling in 2009 was collected from KL1 data history. Turbine under operation was visually inspected and new photographs were clicked during plant shut-down with the help of technical team of KL1 HPS. Measurement of bucket thickness, width and profile along with the comparison with drawing and installed turbine. Proper measurement of runner eroded bucket were noted under instruction and guidance of technical team of KL1 HPS. Dimensional drawing and suitable tools like Vernier calliper, micrometer screw gauge, profile gauge and filler gauge were used. Marking the cavitation prone area of bucket. Spare Pelton runner (after proper overhauling) at power house was also visually inspected and measurement were noted. Visual comparison of photographs shorted during 2009 and 2021 were done and noted the patterns of erosion due to cavitation. Erosion affected area as per KL1 Operation & Maintenance Manual were marked properly. Pattern of cavitation on runner bucket was mostly appearing at splitter nose back side zone along with the rim surface. Similarly photograph of Puwa Khola HPS operating with Pelton turbine were also included and noted pattern of erosion due to pitting mostly on bucket profile. As measurement work was rigorous so sample two buckets were only measured for this study assuming similar wear occurrence in almost nineteen buckets of runner.



(Source: Site visit 2021)

Figure 3.2: Erosion due to sand particle and cavitation (left Puwakhola HPS) and erosion due to cavitation (right KL1HPS) in bucket



(Source: Site visit 2021)

Figure 3.3: After few years run minor effect of cavitation



(Source: Site visit 2021)

Figure 3.4: On long run, tip erosion due to cavitation

3.7 Computational model development for Pelton runner bucket

All the dimensional data and material composition of Pelton turbine assembly was collected from the Kulekhani First HPS Manual and as built drawings. Model was created in CATIA as per the given dimensions and arrangements.

3.8 CFD Model Formulation

To study the runner by CFD analysis, ANSYS Fluent was used. For two dimensional analysis, a cross section of the nozzle and bucket was modelled and meshed. The major purpose of numeric simulation was to determine if there are any low pressure region formation due course of flow that promotes the cavitation phenomenon. After importing the modelled system in Design Modeller, further modifications on the geometry was done and appropriate boundary conditions were defined. The boundary condition used is shown in figure 3.2.

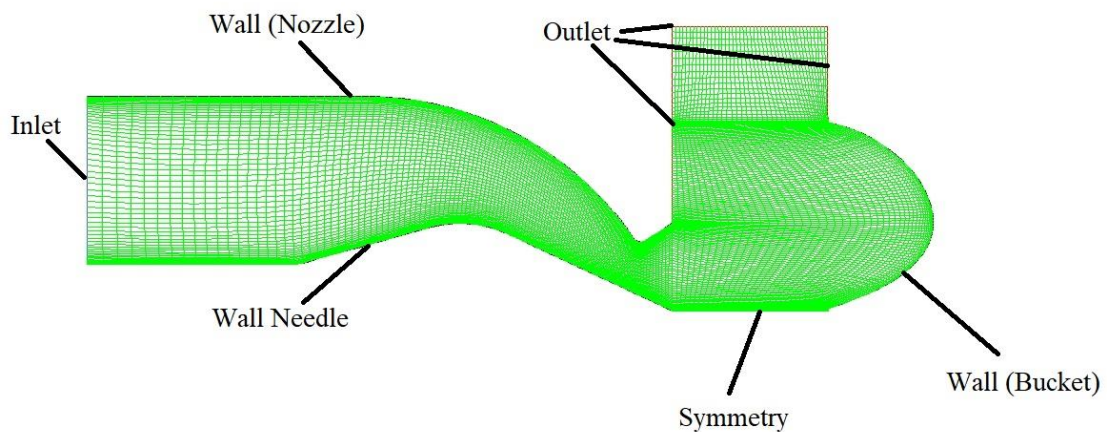


Figure 3.2: Boundary Conditions

Meshing is defined as the process of dividing the whole domain into number of elements so that whenever the input condition is applied on the domain it distributes the load uniformly. For purpose of reducing the calculation time, only a section of flow was modelled and meshed using ICEM CFD. Similar meshing conditions were thus adopted for all simulations. The overview of the basic setup used for all simulations are shown in below:

Table 3.3: Overview of the basic setup

Solver	ANSYS Fluent 18.2
Time discretization	Steady State
Discretization scheme	Second Order
Turbulence model	RNG K- ϵ
Surface tension model	Continuum Surface Force (primary fluid ! water)
Surface tension coefficient	$\sigma_1 = 0.7$ and $\sigma_2 = 0.0728$, [N/m]
Convergence criteria	RMS, Scaled residual target = 10^{-4}
Hardware	Processor: Intel Core i5 @ 3.2 GHz (4 cores). Memory: 24 GB

3.9 Estimations

Estimating the current efficiency of turbine and comparing with the standard efficiency marked ahead by analysing the 12 year operational data like total generation, total running hours and volume of reservoir. Validating the result with application of derived mathematical expression by various researcher regarding efficiency reduction. Generation loss due efficiency reduction. Material removal determination of Pelton turbine bucket.

CHAPTER FOUR: RESULTS AND DISCUSSION

4.1 Generation record of KL1HPS

The monthly total power generation (MWh) since commissioning of plant in FY 2038/39 to recent FY 2077/78 of KL1HPS were extracted from the history data record as presented in appendix A, table 5.1 are plotted to withdraw general bar chart.

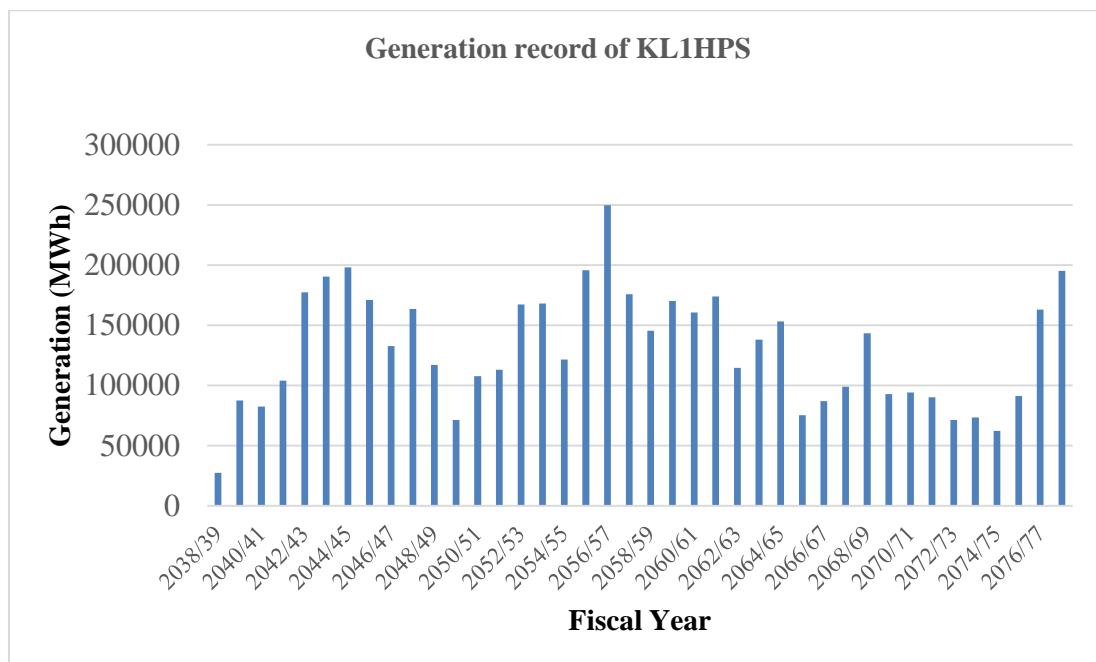


Figure 4.1: Annual generation since commissioning till FY2077/78

The figure 4.1 clearly shows that total generation is highest in FY2056/57 and has fluctuating trend line. From FY 2068/69 to 2075/76 has falling order and during last two fiscal year generation is rapidly increasing order due to heavy rain fall before monsoon and in monsoon season resulting twice evacuation of reservoir and hence more power generation.

4.2 Annual generation and water level of KL1HPS

The historical series of data of annual generation and reservoir water level since FY 2038/39 to FY2077/78 were extracted as in appendix A, table 5.2 to compare the present volume of feed water to harness amount of power generation.

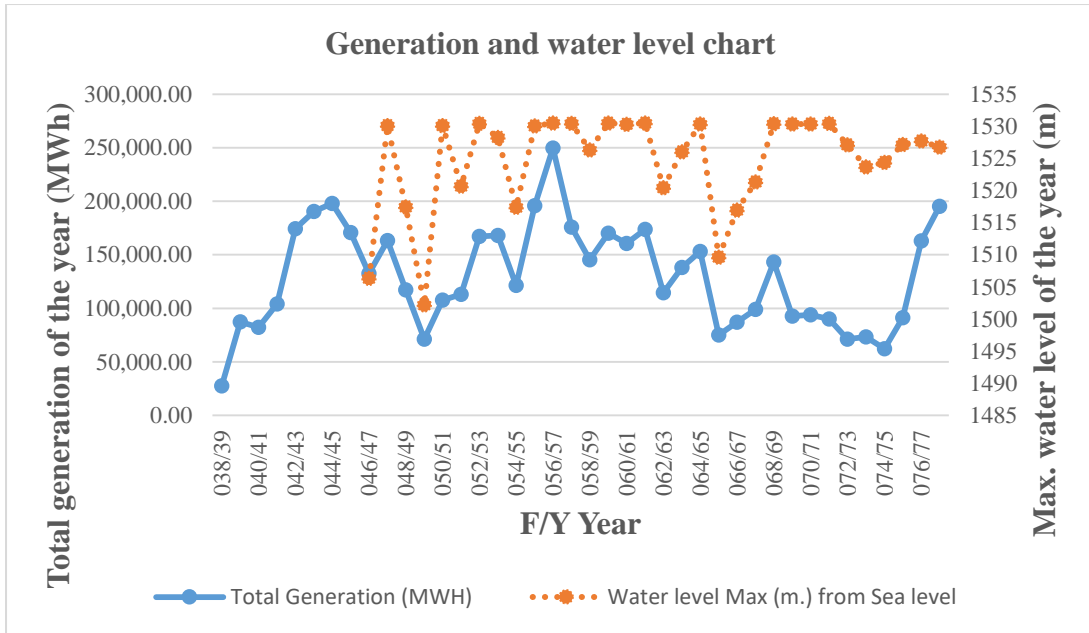


Figure 4.2: Generation and water level chart

The figure 4.2 presented above clearly shows that the highest reservoir level was achieved in FY2056/57 along with highest power generation. During the FY 068/69 to FY071/72 the reservoir water level are about same but the yearly generation has falling trend line indicating higher volume of feed water but still low power generation.

4.3 Annual reservoir water level of KL1HPS

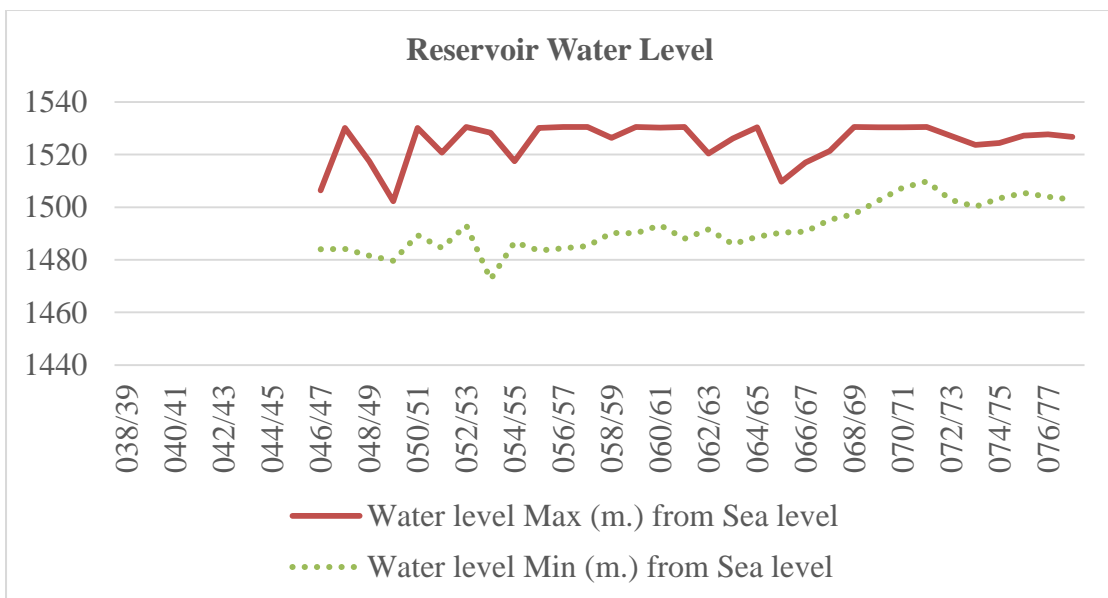


Figure 4.3: Annual max. & min. reservoir water level of KL1HPS

Reservoir water level is in declining order prior to commissioning due to regular sedimentation and deposition at the bed level of reservoir. After FY 2071/72 the highest water level achieved is below the mark level i.e. 1530 m.

4.4 Efficiency calculations

The daily reservoir water level at beginning (RWL_1) of machine start time and reservoir water level at stop time (RWL_2) were noted. The respective volume of water were determined by using the reservoir capacity equation based on polynomial method. The difference ($RWL_1 - RWL_2$) of reservoir water level were executed to determine the volume of water outflow (Q) form the reservoir to the turbine for power generation along with associated effective head (H). Water density considered was 1000 kg/m^3 and gravity $9.8 \text{ m}^2/\text{s}$. Thus calculated the efficiency by employing the general formula as per equation number 1.2 stated above in various data of dry season when machine was operating under full load. The efficiency calculations spreadsheet is presented in appendix A, table5.3.

4.5 Efficiency trend line

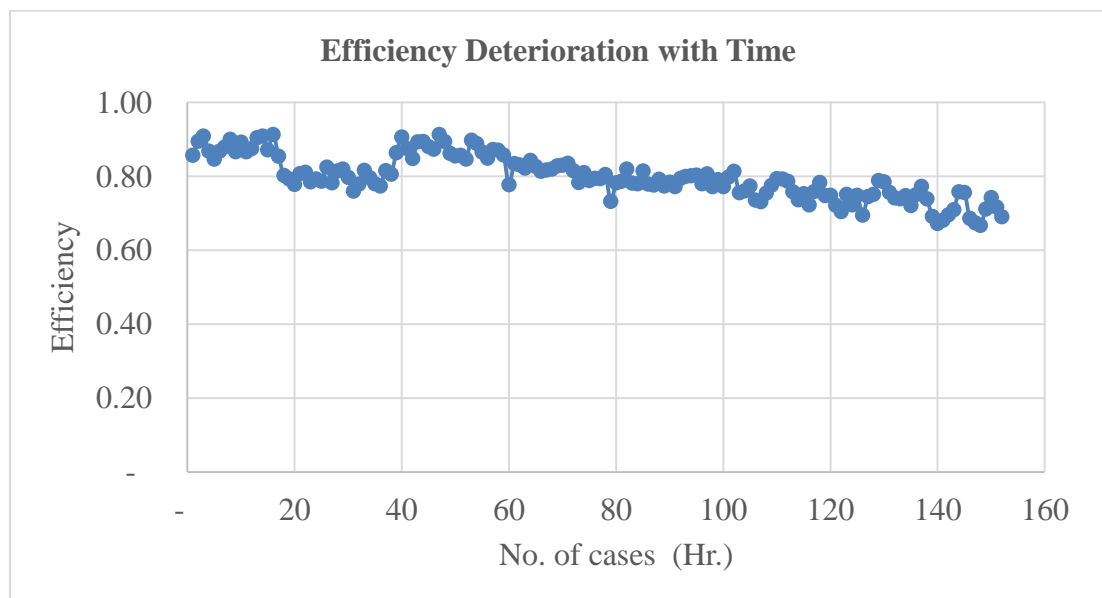


Figure 4.4: Efficiency deterioration trend line

The plot of efficiency of various time data in the figure 4.4 above has a falling trend line. Here time data in X-axis represents the series of dry season data since FY

2072/73 to FY2077/78. It is found that the highest and lowest efficiency achieved are 94% and 67% respectively. Also it is clearly seen that the efficiency is deteriorating day by day.

4.6 Volume of water outflow during machine operations

The volume of outflow water to the turbine for power generation as per running duration on various date of dry season were calculated as in appendix A, table 5.3. The value of volume of feed water to turbine and running hour durations were plotted in Y-axis whereas the various date dry season data along X-axis to determine pattern of the feed water to turbine as in figure 4.5. From the figure during operation for five hour, the volume of water outflow from the reservoir is in incremental trend line.

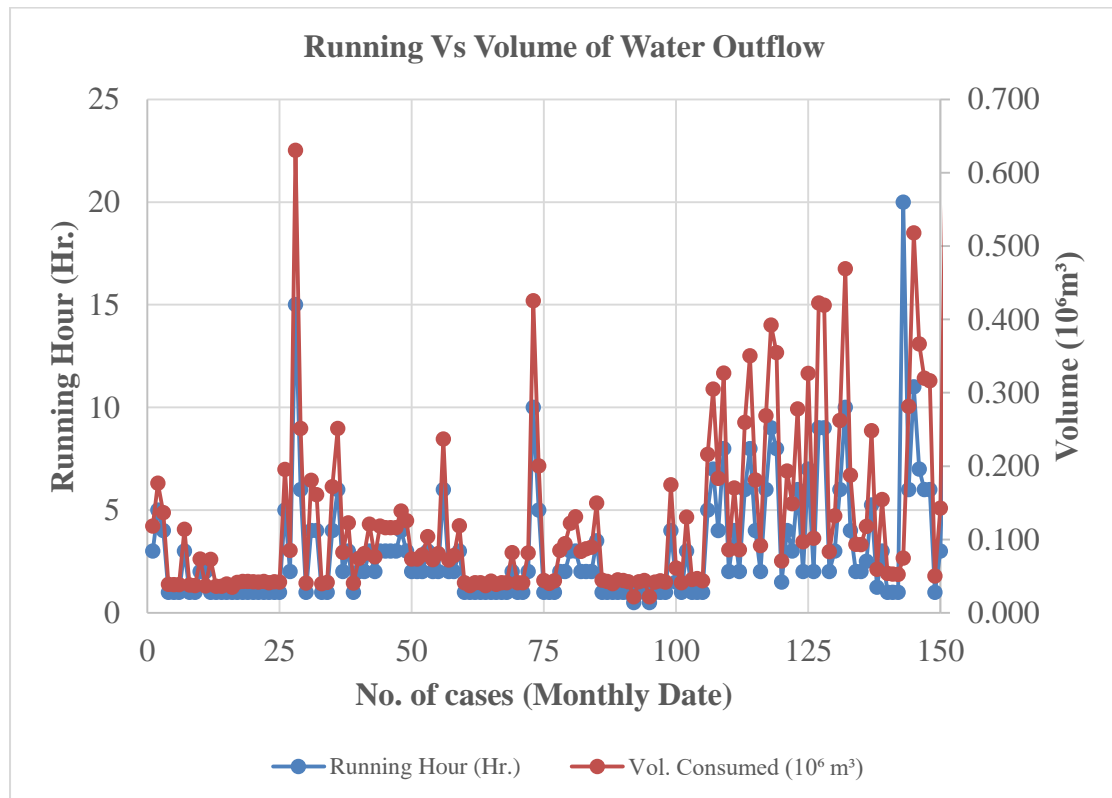


Figure 4.5: Reservoir outflow to turbine

4.7 Volume of water inflow during machine stop

The volume of water inflow to the reservoir when the machine were on stop condition on various date of dry season were calculated as per appendix A, table 5.4. The

obtained value of water inflow along with the duration of machine stop were plotted to Y-axis whereas various date dry season data on X-axis to determine the pattern of water inflow to reservoir as in the figure 4.6 below. The inflows are in fluctuation manner as per inflows from the tributary rivers and catchment area of reservoir.

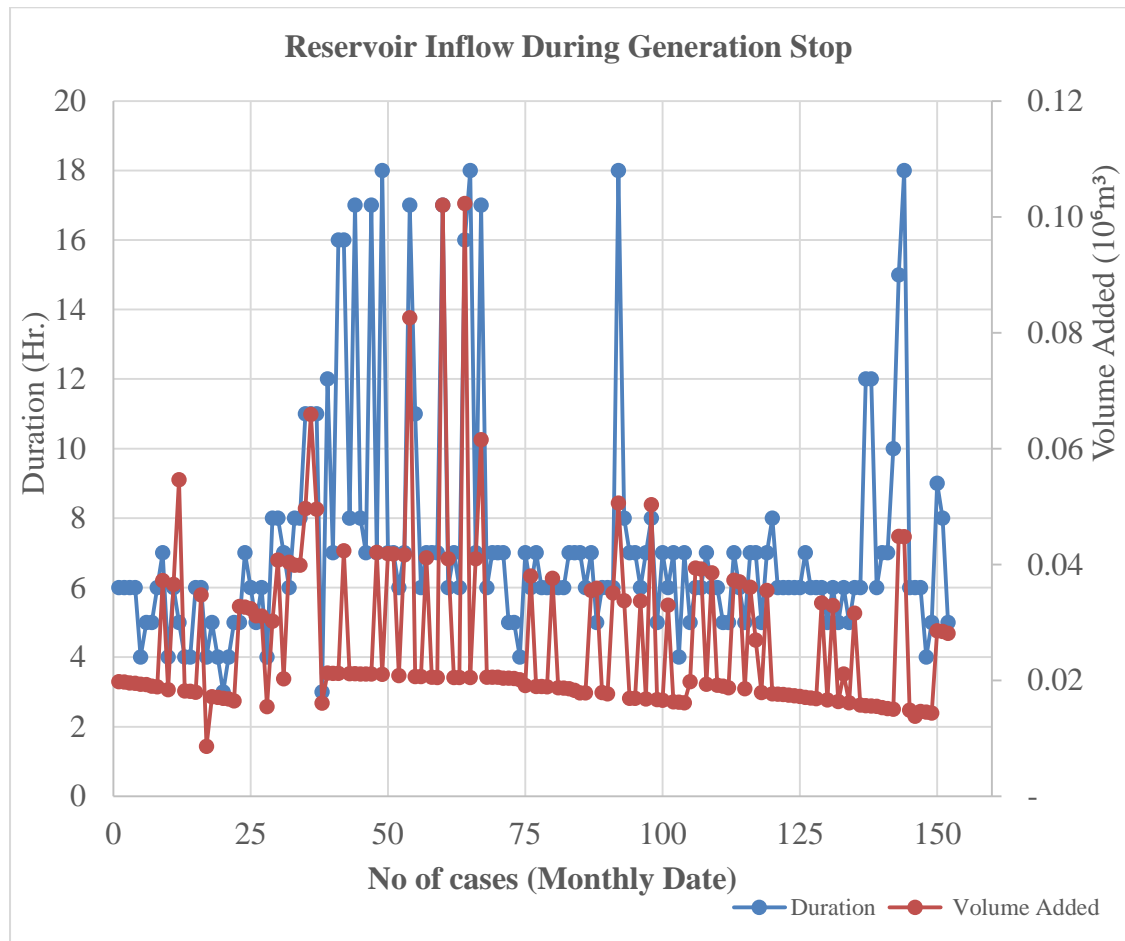


Figure 4.6: Volume of water inflow to reservoir

4.8 Measurements

On the basis of salient features and dimensional drawing measurement of runner installed at powerhouse were carried out during shut-down period. The general suitable tools used for measurement were Vernier calliper, Screw gauge micrometre, Profile gauge set (4 Nos.) and Filler gauge set available at Kulekhani First Hydropower Station, under instruction and guidance of technical team. As it is rigorous to measure installed runner so two sample buckets were only measure among

nineteen buckets of each unit. The noted measurements reading are shown below in tabular form:

Table 4.1: Unit-2 Runner bucket (measurement)

Position (Sample-1)	T1	T2	T3	T4	T5	Maximum wear	Final wear
Section-2	1.6	2.5	0.55	0.95	1.8	3.2	5.05
Section-4	2.3	3	3.2	2.9	0.4		
Section-6	2.1	2.2	2.05	1.45	1.05		
Section-8	2.25	2.4	2.15	0.95	0.95		
Position (Sample-2)	T1	T2	T3	T4	T5	5.05	
Section-2	0.95	1.85	2.05	2.2	3.65		
Section-4	1.7	2.4	5.05	4.7	2.5		
Section-6	0.5	0.8	1.5	1.65	1.15		
Section-8	2	0.95	0.95	1.3	1.45		

4.9 Wear calculations of bucket profile

Table 4.2: Theoretical calculations

S.N.	Description	Values	Units
1	Total generation (MWh) of KL1 till 2077/78	5,213,564.00	MWh
2	Individual Unit generation (Each Unit generate equal quantity.)	2,606,782.00	MWh
3	In a year number of hour	8760	Hr.
4	Unit 30 MW can generate yearly (30 MW ×8760 h)	262800	MWh
5	Total running hour of machine (8760×2606782/262800)	86892.7333	Hr.
6	Upon operation of 86892.733 hr wear is about	5.05	mm
7	Yearly (8760 hr) wear	0.5091	mm
8	Wear (Per 1000 hr)	0.0581	mm

4.10 Erosion analysis

There are various standard erosion models on turbines due to sediment led flow along with their correlations withdrawn and published by professional researchers. Among the various wear models and correlations, sand led erosion in Pelton runner bucket by (Tri Ratna Bajracharya et al., 2007) is executed for this thesis work. The equation is as follows:

Here, in the case of KL1HPS

Quartz content = 63%

Therefore, $a = 1199.8$ and $b = 1.8025$, for quartz content of 60%

Sediment size = 0.001 mm

Erosive wear rate = $1199.8 (0.001)^{1.8025}$

Erosive wear rate = 0.0046 mm/year

Now,

Total Erosion observed: 5.05 mm

Yearly erosion (A): 0.5091 mm

Erosion contribution due to sand particles (B): 0.0046 mm/year

Erosion contribution due to cavitation only (C = A-B): 0.5045 mm/year

Hence on a long run basis, cavitation effect is pronounced on the runner.

4.11 Comparison of sand led and sand free flow in Pelton turbine

Puwakhola hydropower station is a run-off-river (ROR) plant of 6.2 MW capacity installed with horizontal Pelton turbine under NEA. As the river flow is sand led, on long run, the erosion due to pitting phenomena were mainly observed on the surface of buckets. Conversely in the case of storage hydropower plant KL1HPS installed with vertical Pelton turbine of 60 MW capacity, the flow is sand free to higher extent and erosion of bucket surface were mainly due to cavitation were noticed. Thus Pelton turbine operation under sand led and sand free conditions have different erosion phenomena though synergic effects are inherent.

4.12 CFD Modelling

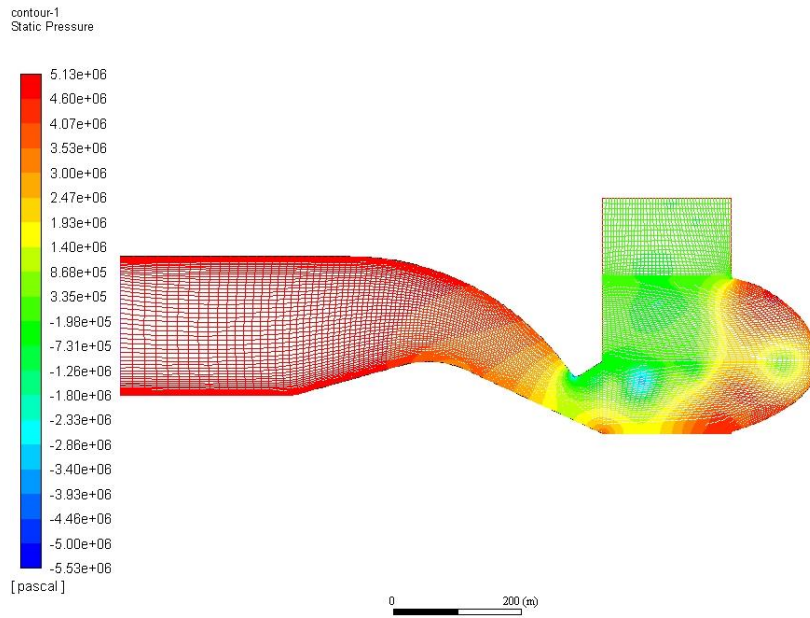


Figure 4.7: Pressure contour in flow domain

On the nozzle outlet, there is a region of low pressure (Blue region), it can be inferred that local boiling of water occurs in this region and there is bubble formation. These bubble travel (as seen in figure 4.7) with high speed jet and gets collapsed in bucket causing pitting due to cavitation.

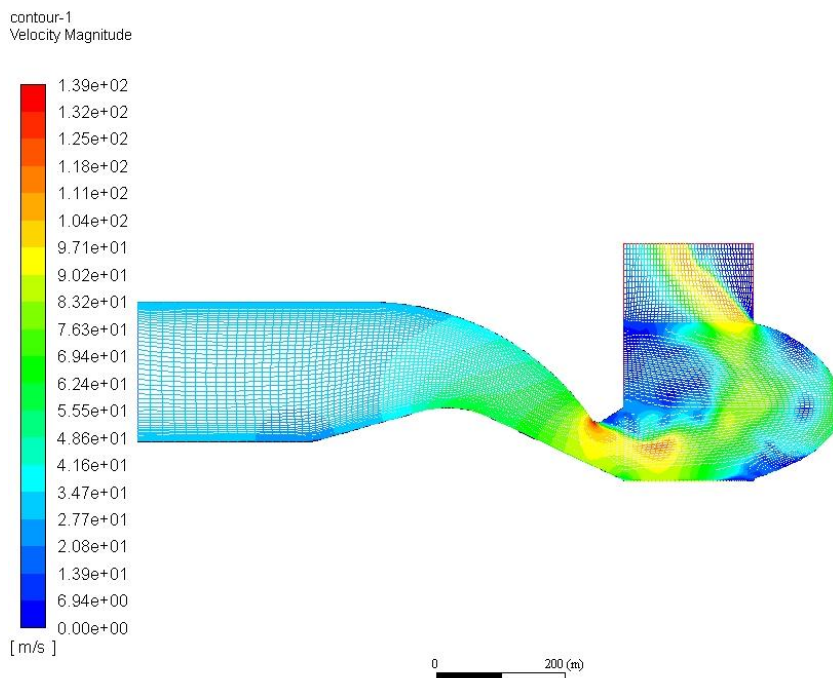


Figure 4.8: Velocity contour in flow domain

From figure 4.8, Velocity of flow from CFD Simulation was seen to be 104 m/s on average in jet flow at exit from nozzle. And with theoretical calculations, velocity of the Jet = 101.8 m/s. With this, error in CFD Calculation is 2.16%.

CHAPTER FIVE: CONCLUSIONS AND RECOMMENDATIONS

5.1 Conclusions

On completion of this research following conclusions are withdrawn:

- Water consumption trend of Pelton turbine generating units on long run was done. It was seen that on long run, due to efficiency deterioration, there is increase in water consumption trend.
- Erosion rate of Pelton turbine of Kulekhani -1 HPS was done. It was seen that total erosion of 0.5091 mm per year was observed of which sand particles only contributed about 0.0046 mm per year. Hence, erosion due to cavitation is pronounced on long run in storage type Pelton runner.
- From CFD analysis (2D, Steady State), analyzing the static pressure distribution, it was seen that there is low pressure region at nozzle outlet. The pressure in the region is very low (negative) and water in that region boils forming a bubble which transfers along with the jet and few of the bubbles collapse in the bucket causing cavitation.

5.2 Recommendations

This research thesis work also put forward the following useful recommendations:

- Plant efficiency is in declining order thus overhaul is required to maintain desire efficiency.
- Regular monitoring and repair of minor erosions and wear can enhance life of runner.
- Power generation at higher head range are beneficial as higher efficiency are achieved.
- Recording of surface erosion of turbine will be helpful in predicting overhauling time of turbine.
- 3D Modelling & CFD simulation may furnish more insightful knowledge.

REFERENCES

1. Bajracharya, T. R., Acharya, B., Joshi, C. B., Saini, R. P., & Dahlhaug, O. G. (2008). Sand erosion of Pelton turbine nozzles and buckets: A case study of Chilime Hydropower Plant. *Wear*, 264(3–4), 177–184. <https://doi.org/10.1016/j.wear.2007.02.021>
2. Bajracharya, Tri Ratna, Saini, R. P., & Dahlhaug, O. G. (2007). Correlation between Sand Led Erosion of Pelton Buckets and Efficiency Losses in High Head Hydropower Schemes. October.
3. Dealing with Sediment: Effects on Dams and Hydropower Generation | Hydro Review. (n.d.). Retrieved July 13, 2021, from <https://www.hydroreview.com/world-regions/dealing-with-sediment-effects-on-dams-and-hydropower-generation/?fbclid=IwAR2HhQBALapSN18pq9OJIaiMnlZdr3Gbvxi-dWuAaJc-Q9s1ekbUHlzMqI>
4. Department of Electricity Development. (2018). Guidelines for Study Of Hydropower Projects. 306. <https://www.doed.gov.np/storage/listies/December2019/guidelines-for-study-of-hydropower-projects-2018.pdf>
5. Gummer, B. J. H. (2018). Combating Silt Erosion in Hydraulic Turbines. 1, 1–14.
6. Hussian, Z., Abdullah, Z., & Alimuddin, Z. (2008). Basic Fluid Mechanics and Hydraulic Machines. <https://books.google.com/books?id=FABEAQAIAAJ&pgis=1>
7. ISO 14026. (2014). International Standard International Standard. In 61010-1 © Iec:2001 (Vol. 2014).
8. Jošt, D., Škerlavaj, A., Pirnat, V., Morgut, M., & Nobile, E. (2019). Detailed analysis of flow in two pelton turbines with efficiency and cavitation prediction. *International Journal of Fluid Machinery and Systems*, 12(4), 388–399. <https://doi.org/10.5293/IJFMS.2019.12.4.388>
9. Neopane, H. P. (2010). Sediment erosion in hydro turbines. Ph.D. Thesis, March, 1–201. <http://ntnu.diva->

portal.org/smash/get/diva2:326677/FULLTEXT01

10. Neopane, H. P., Gunnar Dahlhaug, O., & Cervantes, M. (2011). Sediment Erosion in Hydraulic Turbines. *Global Journal of Researches in Engineering Mechanical and Mechanics Engineering*, 6, 17–26.
11. Nepal Electricity Authority:: *नेपालबिधुतप्राधिकरण*. (n.d.). Retrieved September 17, 2021, from <https://nea.org.np/>
12. Padhy, M. K., & Saini, R. P. (2009). Effect of size and concentration of silt particles on erosion of Pelton turbine buckets. *Energy*, 34(10), 1477–1483. <https://doi.org/10.1016/j.energy.2009.06.015>
13. Poudel, L., Thapa, B., Shrestha, B., & Shrestha, N. (1970). Sediment Impact On Turbine Material: Case Study Of Modi River, Nepal. *Kathmandu University Journal of Science, Engineering and Technology*, 8(1), 88–96. <https://doi.org/10.3126/kuset.v8i1.6047>
14. Rai, A. K., Kumar, A., & Staubli, T. (2017). Hydro-abrasive erosion in Pelton buckets: Classification and field study. *Wear*, 392–393(April), 8–20. <https://doi.org/10.1016/j.wear.2017.08.016>
15. Rossetti, A., Pavesi, G., Ardizzon, G., & Santolin, A. (2014). Numerical analyses of cavitating flow in a pelton turbine. *Journal of Fluids Engineering, Transactions of the ASME*, 136(8), 1–10. <https://doi.org/10.1115/1.4027139>
16. Sangroula, D. P. (1970). Hydropower Development and Its Sustainability With Respect to Sedimentation in Nepal. *Journal of the Institute of Engineering*, 7(1), 56–64. <https://doi.org/10.3126/jie.v7i1.2063>
17. Senapati, P., Rakeshsharma, K. R., Padhy, M. K., & Mohanty, U. K. (2017). Quantification of metal loss due to silt erosion under laboratory conditions. *International Journal of Mechanical and Production Engineering Research and Development*, 7(5), 37–50. <https://doi.org/10.24247/ijmperdoct20175>
18. Shrestha, R. (2020). Impact of Reservoir Sedimentation on Hydroelectric Power Generation : Case Study of Kulekhani First Hydropower Station Impact of Reservoir Sedimentation on Hydroelectric Power Generation : Case Study of Kulekhani First Hydropower Station. October.

19. Thapa. (2004). Sand erosion hydropower.
20. Thapa, B., Chaudhary, P., Dahlhaug, O. G., & Upadhyay, P. (2007). Study of Combined Effect of Sand Erosion and Cavitation in Hydraulic Turbines. International Conference on Small Hydropower, October, 22–24.
21. Truscott, G. F. (1972). A literature survey on abrasive wear in hydraulic machinery. *Wear*, 20(1), 29–50. [https://doi.org/10.1016/0043-1648\(72\)90285-2](https://doi.org/10.1016/0043-1648(72)90285-2)
22. Versteeg, H. K., & Malalasekera, W. (1995). An introduction to computational fluid dynamics - the finite volume method. In undefined.
23. Zeng, C. J., Xiao, Y. X., Zhu, W., Yao, Y. Y., & Wang, Z. W. (2015). Numerical simulation of cavitation flow characteristic on Pelton turbine bucket surface. *IOP Conference Series: Materials Science and Engineering*, 72(Forum 4). <https://doi.org/10.1088/1757-899X/72/4/042043>

APPENDIX A: TABLES OF CHAPTER FOUR

Kulekhani First Hydropower Station

Monthly generation (MWh) data sheet

Table 5.1: Annual generation of KL1HPS

FY/Month	Shrawan	Bhadra	Asoj	Kartik	Mangsir	Paush	Magh	Falgun	Chaitra	Baishakh	Jestha	Asar	Total
038/39									11,023	16,411	-	-	27,434
039/40	661	3,318	4,194	2,964	7,462	11,007	12,477	10,932	10,261	10,607	7,958	5,576	87,417
040/41	5,058	3,074	3,636	2,595	7,518	11,681	11,287	9,342	10,263	7,240	5,527	5,072	82,293
041/42	9,047	5,594	4,715	6,154	7,756	13,578	10,601	8,275	9,256	10,608	8,316	10,112	104,012
042/43	12,940	13,222	9,020	8,437	10,020	15,062	18,512	18,999	20,453	15,848	15,866	16,032	174,411
043/44	17,572	15,344	12,146	13,319	14,462	17,260	17,440	19,250	19,206	15,971	12,914	15,511	190,395
044/45	15,831	17,780	14,897	14,478	17,825	18,740	19,192	17,068	16,487	16,402	14,037	15,340	198,077
045/46	16,808	15,482	17,011	12,135	13,273	17,985	15,563	15,431	12,139	10,019	11,219	13,818	170,883
046/47	17,250	18,641	16,134	10,800	12,011	13,251	10,828	8,331	5,902	6,573	7,262	5,611	132,594
047/48	3,358	10,097	11,687	13,194	12,254	25,818	27,183	21,002	15,798	10,598	5,082	7,339	163,410
048/49	7,903	8,981	8,081	6,418	10,551	18,133	19,607	15,286	9,750	4,424	3,352	4,617	117,103
049/50	7,438	5,155	4,659	3,481	5,064	9,951	12,935	9,911	5,329	2,098	2,486	2,785	71,292
050/51	353	-	-	-	-	11,709	19,997	17,296	17,423	25,476	10,929	4,598	107,781
051/52	6,304	4,303	7,044	4,959	11,499	21,778	17,108	15,651	8,803	4,562	4,367	6,670	113,048
052/53	10,845	17,147	11,833	6,492	8,314	13,445	15,550	14,488	26,664	15,781	14,195	12,443	167,197
053/54	9,904	10,694	14,945	11,385	16,612	26,676	26,586	20,735	14,542	10,996	372	4,538	167,985
054/55	7,712	6,714	16,513	7,816	4,436	7,474	15,104	13,610	10,124	9,847	11,336	10,885	121,571
055/56	15,562	31,986	13,346	8,025	13,204	19,380	18,481	16,867	20,205	11,864	7,649	19,168	195,737
056/57	33,355	34,278	21,139	14,836	11,962	19,307	26,333	26,755	20,815	11,148	12,322	17,430	249,680
057/58	9,023	17,107	16,103	9,072	15,161	18,242	24,925	25,096	19,588	5,554	5,717	10,164	175,752

FY/Month	Shrawan	Bhadra	Asoj	Kartik	Mangsir	Paush	Magh	Falgun	Chaitra	Baishakh	Jestha	Asar	Total
058/59	10,551	10,315	8,885	6,617	8,098	15,108	21,475	19,134	20,027	8,026	8,070	9,115	145,421
059/60	12,147	15,542	14,250	8,293	8,106	16,177	30,871	29,963	13,435	8,533	7,189	5,520	170,026
060/61	10,517	9,086	11,329	9,850	9,566	20,508	19,192	19,540	16,577	11,986	9,578	12,880	160,609
061/62	16,627	10,798	11,960	10,665	9,223	18,091	23,347	20,983	18,940	17,813	8,448	6,890	173,785
062/63	7,953	7,188	7,091	5,623	9,062	13,560	17,132	18,371	5,886	6,777	7,012	9,045	114,700
063/64	8,954	7,407	6,348	6,697	12,319	20,838	20,412	10,226	15,124	14,271	9,091	6,361	138,048
064/65	3,742	5,672	15,260	8,382	8,412	16,467	23,738	20,110	21,113	9,013	10,518	10,589	153,016
065/66	10,316	8,097	3,654	2,131	8,295	12,487	6,195	10,214	2,381	3,313	4,421	3,610	75,114
066/67	4,290	4,756	5,156	4,595	6,612	12,642	10,268	9,495	11,040	6,576	5,884	5,682	86,996
067/68	9,633	3,171	4,396	3,927	5,545	9,594	12,680	11,999	17,468	8,149	6,726	5,598	98,886
068/69	7,888	7,611	13,698	8,112	6,866	8,683	13,638	25,823	25,403	17,814	3,884	3,864	143,284
069/70	4,704	2,205	464	1,148	3,958	8,608	8,291	15,504	27,394	10,560	3,630	6,363	92,829
070/71	9,615	3,767	521	2,938	4,051	4,539	9,733	16,711	15,278	20,471	5,986	474	94,084
071/72	39	11	79	3,141	3,642	3,732	9,481	5,494	9,808	24,797	22,614	7,243	90,081
072/73	626	187	221	716	297	5,776	16,038	9,420	13,184	18,442	2,845	3,604	71,356
073/74	3,946	566	256	723	918	6,253	10,743	13,289	14,232	13,226	6,141	3,109	73,402
074/75	860	313	202	225	202	4,345	5,283	14,322	12,845	12,669	6,428	4,437	62,131
075/76	4,480	2,894	2,209	1,349	2,249	5,878	5,390	2,710	13,504	20,932	16,616	12,973	91,184
076/77	34,087	10,136	6,239	11,710	17,176	13,628	10,978	5,655	7,788	8,934	18,230	18,411	162,972
077/78	32,949	21,530	14,405	13,080	10,499	17,693	16,581	4,014	13,267	6,840	13,147	31,152	195,157

Annual generation and water level

Table 5.2: Annual generation and water level of KL1HPS

FY/Month	Total generation (MWH)	Water level max (m.) from sea level	Water level min (m.) from sea level
038/39	27,434.00		
039/40	87,417.00		
040/41	82,293.00		
041/42	104,012.00		
042/43	174,411.00		
043/44	190,395.00		
044/45	198,077.00		
045/46	170,883.00		
046/47	132,594.00	1,506.33	1,484.06
047/48	163,410.00	1,530.08	1,484.12
048/49	117,103.00	1,517.47	1,481.52
049/50	71,292.00	1,502.19	1,479.57
050/51	107,781.00	1,530.08	1,489.35
051/52	113,048.00	1,520.69	1,484.55
052/53	167,197.00	1,530.47	1,493.18

FY/Month	Total generation (MWH)	Water level max (m.) from sea level	Water level min (m.) from sea level
053/54	167,985.00	1,528.25	1,472.57
054/55	121,571.00	1,517.42	1,486.71
055/56	195,737.00	1,530.06	1,483.50
056/57	249,680.00	1,530.49	1,484.32
057/58	175,752.00	1,530.46	1,485.28
058/59	145,421.00	1,526.31	1,490.27
059/60	170,026.00	1,530.48	1,490.08
060/61	160,609.00	1,530.28	1,493.13
061/62	173,785.00	1,530.48	1,487.98
062/63	114,700.00	1,520.43	1,491.60
063/64	138,048.00	1,526.03	1,485.91
064/65	153,016.00	1,530.36	1,488.74
065/66	75,114.00	1,509.64	1,490.37
066/67	86,996.00	1,516.96	1,490.75
067/68	98,886.00	1,521.34	1,495.22
068/69	143,284.00	1,530.42	1,497.33
069/70	92,829.00	1,530.34	1,502.52

FY/Month	Total generation (MWH)	Water level max (m.) from sea level	Water level min (m.) from sea level
070/71	94,084.00	1,530.36	1,507.32
071/72	90,081.00	1,530.44	1,509.77
072/73	71,356.00	1,527.10	1,502.73
073/74	73,402.00	1,523.67	1,500.24
074/75	62,131.00	1,524.38	1,503.34
075/76	91,184.00	1,527.17	1,505.43
076/77	162,972.00	1,527.70	1,503.96
077/78	195,157.00	1,526.74	1,502.85

Efficiency calculations

Table 5.3: Efficiency spreadsheet

Change in reservoir water volume during machine operation : $Q_{\text{Reservoir}}$								
Reservoir water volume inflow on that day : Q_{Add}								
Effective head of machine operation at instant : H_{Eff}								
Level of bottom floor of turbine (masl) :				950				
Assumption parameters.		Calculations						
1. Water density (kg/m ³)	1000	$Q_{\text{Add}} = Q_{\text{Reservoir}} + Q_{\text{Gen.}} + Q_{\text{Gate (or Q Spill)}}$						
2. Gravity (m/s ²)	9.81							
3. No temperature change								
Case No.	Power	$Q_{\text{Reservoir}}$	Q_{Add}	Q_{Spill}	Q_{Gen}	H_{Eff}	Efficiency	Remarks
1	60	-10.95	0.91	-	11.87	601.29	0.89	
2	60	-10.45	0.91	-	11.36	601.1	0.93	
3	60	-10.29	0.91	-	11.2	600.71	0.94	
4	60	-10.82	0.9	-	11.72	600.63	0.9	
5	60	-10.69	1.34	-	12.03	600.02	0.88	
6	60	-10.67	1.07	-	11.74	599.92	0.9	
7	60	-10.54	1.06	-	11.59	599.26	0.91	
8	60	-10.47	0.87	-	11.34	598.9	0.93	
9	60	-10.32	1.48	-	11.8	598.16	0.9	

Change in reservoir water volume during machine operation : $Q_{\text{Reservoir}}$								
Reservoir water volume inflow on that day : Q_{Add}								
Effective head of machine operation at instant : H_{Eff}								
Level of bottom floor of turbine (masl) :			950					
Assumption parameters.		Calculations						
1. Water density (kg/m ³)	1000	$Q_{\text{Add}} = Q_{\text{Reservoir}} + Q_{\text{Gen.}} + Q_{\text{Gate (or Q Spill)}}$						
2. Gravity (m/s ²)	9.81							
3. No temperature change								
Case No.	Power	$Q_{\text{Reservoir}}$	Q_{Add}	Q_{Spill}	Q_{Gen}	H_{Eff}	Efficiency	Remarks
10	60	-10.18	1.28	-	11.46	597.46	0.92	
11	60	-10.12	1.69	-	11.81	597.15	0.9	
12	60	-8.66	3.04	-	11.7	597.06	0.9	
13	60	-10.06	1.26	-	11.33	596.85	0.93	
14	60	-10.02	1.26	-	11.28	596.62	0.94	
15	60	-10.93	0.83	-	11.76	596.18	0.9	
16	60	-9.65	1.61	-	11.26	594.68	0.94	
17	60	-11.44	0.6	-	12.04	594.08	0.88	
18	60	-11.88	0.95	-	12.83	593.91	0.83	
19	60	-11.81	1.18	-	12.99	593.63	0.82	
20	60	-11.68	1.56	-	13.25	593.08	0.8	
21	60	-11.6	1.17	-	12.77	592.72	0.84	

Change in reservoir water volume during machine operation : $Q_{\text{Reservoir}}$								
Reservoir water volume inflow on that day : Q_{Add}								
Effective head of machine operation at instant : H_{Eff}								
Level of bottom floor of turbine (masl) :			950					
Assumption parameters.			Calculations					
1. Water density (kg/m ³)		1000		$Q_{\text{Add}} = Q_{\text{Reservoir}} + Q_{\text{Gen.}} + Q_{\text{Gate (or Q Spill)}}$				
2. Gravity (m/s ²)		9.81						
3. No temperature change								
Case No.	Power	$Q_{\text{Reservoir}}$	Q_{Add}	Q_{Spill}	Q_{Gen}	H_{Eff}	Efficiency	Remarks
22	60	-11.82	0.91	-	12.73	591.69	0.84	
23	60	-11.34	1.82	-	13.16	591.57	0.81	
24	60	-11.74	1.29	-	13.03	591.36	0.82	
25	60	-11.65	1.5	-	13.15	590.98	0.81	
26	60	-10.85	1.73	-	12.58	589.39	0.85	
27	60	-11.83	1.44	-	13.27	588.97	0.81	
28	60	-11.68	1.07	-	12.75	588.62	0.84	
29	60	-11.63	1.05	-	12.68	588.14	0.85	
30	60	-11.31	1.41	-	12.72	603.02	0.82	
31	60	-12.55	0.8	-	13.35	602.58	0.79	
32	60	-11.16	1.87	-	13.03	602.33	0.81	
33	60	-11.06	1.39	-	12.45	601.83	0.84	

Change in reservoir water volume during machine operation : $Q_{\text{Reservoir}}$								
Reservoir water volume inflow on that day : Q_{Add}								
Effective head of machine operation at instant : H_{Eff}								
Level of bottom floor of turbine (masl) :			950					
Assumption parameters.		Calculations						
1. Water density (kg/m ³)	1000	$Q_{\text{Add}} = Q_{\text{Reservoir}} + Q_{\text{Gen.}} + Q_{\text{Gate (or Q Spill)}}$						
2. Gravity (m/s ²)	9.81							
3. No temperature change								
Case No.	Power	$Q_{\text{Reservoir}}$	Q_{Add}	Q_{Spill}	Q_{Gen}	H_{Eff}	Efficiency	Remarks
34	60	-11.52	1.39	-	12.91	594.44	0.82	
35	60	-11.94	1.25	-	13.2	594.18	0.81	
36	60	-11.63	1.66	-	13.29	593.87	0.8	
37	60	-11.42	1.25	-	12.67	591.93	0.84	
38	60	-11.34	1.49	-	12.82	591.57	0.83	
39	60	-11.2	0.49	-	11.69	605.28	0.89	
40	60	-10.3	0.84	-	11.14	605.23	0.94	
41	60	-11.18	0.37	-	11.55	605.2	0.9	
42	60	-11.17	0.74	-	11.91	605.16	0.88	
43	60	-10.57	0.73	-	11.31	605.1	0.92	
44	60	-10.95	0.35	-	11.3	605.04	0.92	
45	60	-10.75	0.73	-	11.48	604.99	0.91	

Change in reservoir water volume during machine operation : $Q_{\text{Reservoir}}$								
Reservoir water volume inflow on that day : Q_{Add}								
Effective head of machine operation at instant : H_{Eff}								
Level of bottom floor of turbine (masl) :			950					
Assumption parameters.		Calculations						
1. Water density (kg/m ³)	1000	$Q_{\text{Add}} = Q_{\text{Reservoir}} + Q_{\text{Gen.}} + Q_{\text{Gate (or Q Spill)}}$						
2. Gravity (m/s ²)	9.81							
3. No temperature change								
Case No.	Power	$Q_{\text{Reservoir}}$	Q_{Add}	Q_{Spill}	Q_{Gen}	H_{Eff}	Efficiency	Remarks
46	60	-10.73	0.84	-	11.57	604.92	0.9	
47	60	-10.72	0.34	-	11.07	604.88	0.94	
48	60	-9.64	1.67	-	11.31	604.8	0.92	
49	60	-11.64	0.09	-	11.73	604.61	0.89	
50	60	-10.16	1.66	-	11.82	604.47	0.88	
51	60	-10.14	1.66	-	11.8	604.38	0.89	
52	60	-10.98	0.96	-	11.95	604.23	0.88	
53	60	-9.62	1.65	-	11.27	604.15	0.93	
54	60	-10.04	1.35	-	11.39	603.79	0.92	
55	60	-11.18	0.52	-	11.7	603.78	0.89	
56	60	-10.97	0.96	-	11.93	603.69	0.88	
57	60	-9.98	1.63	-	11.61	603.5	0.9	

Change in reservoir water volume during machine operation : $Q_{\text{Reservoir}}$								
Reservoir water volume inflow on that day : Q_{Add}								
Effective head of machine operation at instant : H_{Eff}								
Level of bottom floor of turbine (masl) :			950					
Assumption parameters.			Calculations					
1. Water density (kg/m ³)		1000		$Q_{\text{Add}} = Q_{\text{Reservoir}} + Q_{\text{Gen.}} + Q_{\text{Gate (or Q Spill)}}$				
2. Gravity (m/s ²)		9.81						
3. No temperature change								
Case No.	Power	$Q_{\text{Reservoir}}$	Q_{Add}	Q_{Spill}	Q_{Gen}	H_{Eff}	Efficiency	Remarks
58	60	-10.82	0.81	-	11.64	603.42	0.9	
59	60	-11	0.81	-	11.81	603.34	0.89	
60	60	-11.36	1.67	-	13.03	603.28	0.8	
61	60	-10.24	1.9	-	12.14	603.37	0.86	
62	60	-11.38	0.81	-	12.19	603.36	0.86	
63	60	-11.37	0.95	-	12.32	603.32	0.85	
64	60	-10.24	1.78	-	12.01	603.33	0.87	
65	60	-11.94	0.32	-	12.25	603.32	0.85	
66	60	-10.82	1.63	-	12.45	603.4	0.84	
67	60	-11.39	1	-	12.4	603.41	0.85	
68	60	-11.41	0.95	-	12.36	603.49	0.85	
69	60	-11.41	0.82	-	12.22	603.5	0.86	

Change in reservoir water volume during machine operation : $Q_{\text{Reservoir}}$								
Reservoir water volume inflow on that day : Q_{Add}								
Effective head of machine operation at instant : H_{Eff}								
Level of bottom floor of turbine (masl) :			950					
Assumption parameters.		Calculations						
1. Water density (kg/m ³)	1000	$Q_{\text{Add}} = Q_{\text{Reservoir}} + Q_{\text{Gen.}} + Q_{\text{Gate (or Q Spill)}}$						
2. Gravity (m/s ²)	9.81							
3. No temperature change								
Case No.	Power	$Q_{\text{Reservoir}}$	Q_{Add}	Q_{Spill}	Q_{Gen}	H_{Eff}	Efficiency	Remarks
70	60	-11.39	0.81	-	12.2	603.39	0.86	
71	60	-11.32	0.81	-	12.13	603.09	0.86	
72	60	-11.3	1.13	-	12.43	602.96	0.84	
73	60	-11.81	1.13	-	12.94	602.75	0.81	
74	60	-11.13	1.4	-	12.52	602.15	0.84	
75	60	-12.18	0.76	-	12.94	599.52	0.81	
76	60	-11.07	1.76	-	12.83	599.3	0.82	
77	60	-12.1	0.75	-	12.85	599.16	0.82	
78	60	-11.8	0.88	-	12.68	599	0.83	
79	60	-13.07	0.87	-	13.94	598.83	0.76	
80	60	-11.3	1.74	-	13.04	598.73	0.81	
81	60	-12.12	0.87	-	12.98	598.48	0.81	

Change in reservoir water volume during machine operation : $Q_{\text{Reservoir}}$								
Reservoir water volume inflow on that day : Q_{Add}								
Effective head of machine operation at instant : H_{Eff}								
Level of bottom floor of turbine (masl) :			950					
Assumption parameters.		Calculations						
1. Water density (kg/m ³)	1000	$Q_{\text{Add}} = Q_{\text{Reservoir}} + Q_{\text{Gen.}} + Q_{\text{Gate (or Q Spill)}}$						
2. Gravity (m/s ²)	9.81							
3. No temperature change								
Case No.	Power	$Q_{\text{Reservoir}}$	Q_{Add}	Q_{Spill}	Q_{Gen}	H_{Eff}	Efficiency	Remarks
82	60	-11.6	0.86	-	12.47	598.13	0.85	
83	60	-12.12	0.74	-	12.85	608.23	0.81	
84	60	-12.4	0.72	-	13.13	597.15	0.81	
85	60	-11.89	0.71	-	12.6	596.04	0.84	
86	60	-12.34	0.82	-	13.17	595.86	0.81	
87	60	-11.8	1.41	-	13.21	595.66	0.8	
88	60	-10.95	1.99	-	12.94	596.26	0.82	
89	60	-12.42	0.83	-	13.25	596.18	0.8	
90	60	-12.27	0.82	-	13.08	595.55	0.81	
91	60	-11.68	1.62	-	13.3	595.14	0.8	
92	60	-12.19	0.78	-	12.97	593.23	0.82	
93	60	-11.72	1.17	-	12.89	593.23	0.83	

Change in reservoir water volume during machine operation : $Q_{\text{Reservoir}}$								
Reservoir water volume inflow on that day : Q_{Add}								
Effective head of machine operation at instant : H_{Eff}								
Level of bottom floor of turbine (masl) :			950					
Assumption parameters.		Calculations						
1. Water density (kg/m ³)	1000	$Q_{\text{Add}} = Q_{\text{Reservoir}} + Q_{\text{Gen.}} + Q_{\text{Gate (or Q Spill)}}$						
2. Gravity (m/s ²)	9.81							
3. No temperature change								
Case No.	Power	$Q_{\text{Reservoir}}$	Q_{Add}	Q_{Spill}	Q_{Gen}	H_{Eff}	Efficiency	Remarks
94	60	-12.18	0.67	-	12.85	593.22	0.83	
95	60	-12.16	0.67	-	12.83	593.13	0.83	
96	60	-11.66	1.56	-	13.22	592.98	0.81	
97	60	-12.12	0.67	-	12.78	592.93	0.83	
98	60	-11.61	1.75	-	13.36	592.75	0.8	
99	60	-12.12	0.92	-	13.05	592.48	0.82	
100	60	-12.72	0.66	-	13.37	592.1	0.8	
101	60	-11.41	1.53	-	12.94	591.89	0.83	
102	60	-12.06	0.65	-	12.71	591.43	0.84	
103	60	-12.56	1.13	-	13.69	591.03	0.78	
104	60	-12.95	0.64	-	13.59	590.82	0.79	
105	60	-12.05	1.1	-	13.14	601.29	0.8	

Change in reservoir water volume during machine operation : $Q_{\text{Reservoir}}$								
Reservoir water volume inflow on that day : Q_{Add}								
Effective head of machine operation at instant : H_{Eff}								
Level of bottom floor of turbine (masl) :			950					
Assumption parameters.		Calculations						
1. Water density (kg/m ³)	1000	$Q_{\text{Add}} = Q_{\text{Reservoir}} + Q_{\text{Gen.}} + Q_{\text{Gate (or Q Spill)}}$						
2. Gravity (m/s ²)	9.81							
3. No temperature change								
Case No.	Power	$Q_{\text{Reservoir}}$	Q_{Add}	Q_{Spill}	Q_{Gen}	H_{Eff}	Efficiency	Remarks
106	60	-12	1.82	-	13.83	601.1	0.76	
107	60	-12.1	1.82	-	13.91	600.82	0.76	
108	60	-12.72	0.77	-	13.49	600.13	0.78	
109	60	-11.35	1.78	-	13.13	599.96	0.8	
110	60	-11.95	0.89	-	12.84	599.67	0.82	
111	60	-11.82	1.05	-	12.87	599.08	0.82	
112	60	-11.95	1.04	-	12.99	598.51	0.81	
113	60	-12.01	1.48	-	13.49	598.02	0.78	
114	60	-12.17	1.71	-	13.88	597.77	0.76	
115	60	-12.58	1.03	-	13.61	596.83	0.78	
116	60	-12.75	1.43	-	14.18	596.5	0.75	
117	60	-12.44	1.07	-	13.51	596.28	0.78	

Change in reservoir water volume during machine operation : $Q_{\text{Reservoir}}$								
Reservoir water volume inflow on that day : Q_{Add}								
Effective head of machine operation at instant : H_{Eff}								
Level of bottom floor of turbine (masl) :			950					
Assumption parameters.			Calculations					
1. Water density (kg/m ³)		1000		$Q_{\text{Add}} = Q_{\text{Reservoir}} + Q_{\text{Gen.}} + Q_{\text{Gate (or Q Spill)}}$				
2. Gravity (m/s ²)		9.81						
3. No temperature change								
Case No.	Power	$Q_{\text{Reservoir}}$	Q_{Add}	Q_{Spill}	Q_{Gen}	H_{Eff}	Efficiency	Remarks
118	60	-12.1	0.99	-	13.1	596.01	0.81	
119	60	-12.31	1.41	-	13.72	595.73	0.77	
120	60	-13.1	0.61	-	13.71	595.59	0.77	
121	60	-13.41	0.82	-	14.22	595.23	0.75	
122	60	-13.77	0.81	-	14.58	595.05	0.73	
123	60	-12.87	0.81	-	13.67	594.69	0.78	
124	60	-13.43	0.8	-	14.23	594.38	0.75	
125	60	-12.95	0.8	-	13.75	594.12	0.77	
126	60	-14.13	0.68	-	14.81	593.48	0.72	
127	60	-13.03	0.78	-	13.82	593.28	0.77	
128	60	-12.94	0.78	-	13.71	592.9	0.78	
129	60	-11.54	1.54	-	13.09	592.47	0.82	

Change in reservoir water volume during machine operation : $Q_{\text{Reservoir}}$								
Reservoir water volume inflow on that day : Q_{Add}								
Effective head of machine operation at instant : H_{Eff}								
Level of bottom floor of turbine (masl) :			950					
Assumption parameters.			Calculations					
1. Water density (kg/m ³)		1000		$Q_{\text{Add}} = Q_{\text{Reservoir}} + Q_{\text{Gen.}} + Q_{\text{Gate (or Q Spill)}}$				
2. Gravity (m/s ²)		9.81						
3. No temperature change								
Case No.	Power	$Q_{\text{Reservoir}}$	Q_{Add}	Q_{Spill}	Q_{Gen}	H_{Eff}	Efficiency	Remarks
130	60	-12.22	0.92	-	13.14	592.1	0.81	
131	60	-12.14	1.52	-	13.66	591.75	0.78	
132	60	-13.03	0.91	-	13.93	591.44	0.77	
133	60	-13.02	0.98	-	14	591.08	0.76	
134	60	-12.93	0.9	-	13.83	590.74	0.77	
135	60	-12.91	1.46	-	14.37	589.81	0.75	
136	60	-13.08	0.73	-	13.81	589.63	0.78	
137	60	-13.05	0.36	-	13.42	589.38	0.8	
138	60	-13.67	0.36	-	14.03	589.14	0.76	
139	60	-14.3	0.72	-	15.02	588.83	0.71	
140	60	-14.84	0.61	-	15.45	588.27	0.7	
141	60	-14.66	0.6	-	15.26	587.68	0.7	

Change in reservoir water volume during machine operation : $Q_{\text{Reservoir}}$								
Reservoir water volume inflow on that day : Q_{Add}								
Effective head of machine operation at instant : H_{Eff}								
Level of bottom floor of turbine (masl) :			950					
Assumption parameters.		Calculations						
1. Water density (kg/m ³)	1000	$Q_{\text{Add}} = Q_{\text{Reservoir}} + Q_{\text{Gen.}} + Q_{\text{Gate (or Q Spill)}}$						
2. Gravity (m/s ²)	9.81							
3. No temperature change								
Case No.	Power	$Q_{\text{Reservoir}}$	Q_{Add}	Q_{Spill}	Q_{Gen}	H_{Eff}	Efficiency	Remarks
142	60	-14.54	0.42	-	14.96	587.29	0.72	
143	60	-13.84	0.83	-	14.67	587.25	0.73	
144	60	-13.03	0.69	-	13.72	587.08	0.78	
145	60	-13.08	0.69	-	13.77	586.77	0.78	
146	60	-14.55	0.64	-	15.19	586.34	0.71	
147	60	-14.8	0.68	-	15.48	585.9	0.7	
148	60	-14.65	1.01	-	15.65	585.4	0.69	
149	60	-13.88	0.8	-	14.68	585.05	0.74	
150	60	-13.2	0.88	-	14.08	584.98	0.77	
151	60	-13.6	0.99	-	14.58	584.6	0.74	
152	60	-13.58	1.56	-	15.14	584.03	0.71	

Reservoir outflow during machine operation

Water level measured in masl.

Volume of water calculated in million cubic meter.

Table 5.4: Volume of water outflow during machine operations

Case	Month/Year	Date	Load	Machine Start	Machine Stop	Running Hour	Water level at Start	Water level at stop	Average Water Level	Change in water level	Volume of Water (10 ⁶ m ³) at Start	Volume of Water (10 ⁶ m ³) at Stop	Change of Reservoir	Change Rate
1	Poush 73	26	60	17:00	20:00	3:00	1522.69	1522.63	1522.66	0.06	69.84	69.722	-0.118	-10.951
2		27	60	17:00	21:42	4:42	1522.52	1522.43	1522.48	0.09	69.505	69.329	-0.177	-10.447
3		29	60	17:20	21:01	3:41	1522.14	1522.07	1522.11	0.07	68.761	68.625	-0.136	-10.293
4	Magh 73	2	60	19:00	20:00	1:00	1522.04	1522.02	1522.03	0.02	68.566	68.527	-0.039	-10.816
5		6	60	21:00	22:00	1:00	1521.46	1521.44	1521.45	0.02	67.443	67.405	-0.038	-10.693
6		7	60	19:00	20:00	1:00	1521.36	1521.34	1521.35	0.02	67.251	67.212	-0.038	-10.672
7		12	60	18:00	21:00	3:00	1520.75	1520.69	1520.72	0.06	66.086	65.972	-0.114	-10.539
8		16	60	19:00	20:00	1:00	1520.39	1520.37	1520.38	0.02	65.405	65.367	-0.038	-10.468
9		23	60	19:00	20:00	1:00	1519.69	1519.67	1519.68	0.02	64.095	64.058	-0.037	-10.322
10		27	60	19:00	21:00	2:00	1519.03	1518.99	1519.01	0.04	62.877	62.803	-0.073	-10.184
11		29	60	19:00	20:00	1:00	1518.72	1518.7	1518.71	0.02	62.31	62.274	-0.036	-10.122
12		Falgun 73	1	60	18:10	20:30	2:20	1518.65	1518.61	1518.63	0.04	62.183	62.11	-0.073

Case	Month/Year	Date	Load	Machine Start	Machine Stop	Running Hour	Water level at Start	Water level at stop	Average Water Level	Change in water level	Volume of Water (10 ⁶ m ³) at Start	Volume of Water (10 ⁶ m ³) at Stop	Change of Reservoir	Change Rate
13		2	60	19:00	20:00	1:00	1518.44	1518.42	1518.43	0.02	61.801	61.765	-0.036	-10.065
14		3	60	19:00	20:00	1:00	1518.22	1518.2	1518.21	0.02	61.403	61.367	-0.036	-10.02
15		5	60	19:00	20:00	1:00	1517.8	1517.78	1517.79	0.022	60.649	60.61	-0.039	-10.928
16		16	60	7:00	8:00	1:00	1516.37	1516.35	1516.36	0.02	58.128	58.094	-0.035	-9.648
17		18	60	19:00	20:00	1:00	1515.8	1515.78	1515.79	0.024	57.144	57.103	-0.041	-11.441
18		19	60	19:00	20:00	1:00	1515.64	1515.62	1515.63	0.025	56.87	56.827	-0.043	-11.878
19		21	60	8:00	9:00	1:00	1515.37	1515.35	1515.36	0.025	56.409	56.367	-0.043	-11.812
20		23	60	17:00	18:00	1:00	1514.85	1514.83	1514.84	0.025	55.529	55.487	-0.042	-11.685
21		24	60	19:00	20:00	1:00	1514.51	1514.49	1514.5	0.025	54.959	54.917	-0.042	-11.602
22		Chaitra 73	3	60	19:00	20:00	1:00	1513.53	1513.5	1513.52	0.026	53.338	53.296	-0.043
23	4		60	20:00	21:00	1:00	1513.41	1513.39	1513.4	0.025	53.142	53.101	-0.041	-11.337
24	6		60	19:00	20:00	1:00	1513.21	1513.18	1513.2	0.026	52.816	52.774	-0.042	-11.741
25	8		60	19:00	20:00	1:00	1512.85	1512.82	1512.84	0.026	52.233	52.191	-0.042	-11.651
26	25		60	10:00	15:00	5:00	1511.39	1511.27	1511.33	0.125	49.913	49.718	-0.195	-10.848
27	26		60	19:00	21:00	2:00	1510.95	1510.9	1510.92	0.055	49.228	49.143	-0.085	-11.83
28	27		60	9:00:00	0:00	15:00	1510.8	1510.39	1510.6	0.41	48.996	48.366	-0.63	-11.676
29	28		60	8:00	14:00	6:00	1510.22	1510.06	1510.14	0.165	48.106	47.855	-0.251	-11.631
30	Poush 74	19	60	17:00	18:00	1:00	1524.31	1524.29	1524.3	0.02	73.086	73.046	-0.041	-11.307

Case	Month/Year	Date	Load	Machine Start	Machine Stop	Running Hour	Water level at Start	Water level at stop	Average Water Level	Change in water level	Volume of Water (10 ⁶ m ³) at Start	Volume of Water (10 ⁶ m ³) at Stop	Change of Reservoir	Change Rate
31		25	60	17:00	21:00	4:00	1523.93	1523.84	1523.89	0.09	72.316	72.135	-0.181	-12.548
32		26	60	17:00	21:00	4:00	1523.69	1523.61	1523.65	0.08	71.832	71.671	-0.161	-11.165
33	Magh 74	12	60	17:00	18:00	1:00	1523.18	1523.16	1523.17	0.02	70.811	70.771	-0.04	-11.061
34	Chaitra 74	5	60	16:00	17:00	1:00	1516.15	1516.13	1516.14	0.024	57.747	57.706	-0.041	-11.524
35		6	60	12:00	16:00	4:00	1515.94	1515.84	1515.89	0.1	57.385	57.213	-0.172	-11.943
36		12	60	14:00	20:00	6:00	1515.66	1515.51	1515.59	0.147	56.904	56.653	-0.251	-11.631
37		13	60	19:00	21:00	2:00	1513.77	1513.72	1513.75	0.05	53.732	53.65	-0.082	-11.42
38		26	60	9:00	12:00	3:00	1513.44	1513.37	1513.4	0.075	53.191	53.069	-0.122	-11.338
39	Poush 75	2	60	17:00	18:00	1:00	1526.47	1526.45	1526.46	0.019	77.576	77.536	-0.04	-11.197
40		10	60	17:00	19:00	2:00	1526.43	1526.4	1526.41	0.035	77.491	77.417	-0.074	-10.303
41		11	60	17:00	19:00	2:00	1526.4	1526.36	1526.38	0.038	77.428	77.347	-0.08	-11.18
42		12	60	17:00	20:00	3:00	1526.37	1526.31	1526.34	0.057	77.364	77.243	-0.121	-11.171
43		13	60	17:00	19:00	2:00	1526.3	1526.26	1526.28	0.036	77.216	77.14	-0.076	-10.571
44		15	60	17:00	20:00	3:00	1526.26	1526.2	1526.23	0.056	77.131	77.013	-0.118	-10.952
45		16	60	17:00	20:00	3:00	1526.21	1526.16	1526.18	0.055	77.026	76.91	-0.116	-10.747
46		17	60	17:00	20:00	3:00	1526.14	1526.09	1526.11	0.055	76.878	76.762	-0.116	-10.732

Case	Month/Year	Date	Load	Machine Start	Machine Stop	Running Hour	Water level at Start	Water level at stop	Average Water Level	Change in water level	Volume of Water (10 ⁶ m ³) at Start	Volume of Water (10 ⁶ m ³) at Stop	Change of Reservoir	Change Rate
47		18	60	17:00	20:00	3:00	1526.1	1526.05	1526.07	0.055	76.794	76.678	-0.116	-10.724
48		19	60	17:00	21:00	4:00	1526.03	1525.96	1526	0.066	76.646	76.508	-0.139	-9.638
49		20	60	17:00	20:00	3:00	1525.85	1525.79	1525.82	0.06	76.268	76.142	-0.126	-11.643
50		22	60	17:00	19:00	2:00	1525.7	1525.67	1525.68	0.035	75.954	75.881	-0.073	-10.16
51		23	60	17:00	19:00	2:00	1525.62	1525.59	1525.6	0.035	75.787	75.714	-0.073	-10.145
52		25	60	18:00	20:00	2:00	1525.48	1525.44	1525.46	0.038	75.495	75.416	-0.079	-10.985
53		26	60	17:00	20:00	3:00	1525.41	1525.36	1525.39	0.05	75.349	75.246	-0.104	-9.622
54	Magh 75	9	60	18:00	20:00	2:00	1525.06	1525.03	1525.04	0.035	74.624	74.552	-0.072	-10.036
55		14	60	17:00	19:00	2:00	1525.05	1525.01	1525.03	0.039	74.604	74.523	-0.081	-11.181
56		15	60	13:00	19:00	6:00	1525	1524.89	1524.94	0.115	74.5	74.263	-0.237	-10.971
57		17	60	17:00	19:00	2:00	1524.78	1524.75	1524.76	0.035	74.047	73.976	-0.072	-9.982
58		18	60	17:00	19:00	2:00	1524.7	1524.66	1524.68	0.038	73.883	73.805	-0.078	-10.821
59		19	60	8:00	11:00	3:00	1524.64	1524.58	1524.61	0.058	73.76	73.641	-0.119	-10.996
60		26	60	18:00	19:00	1:00	1524.56	1524.54	1524.55	0.02	73.596	73.556	-0.041	-11.362
61	29	60	18:00	19:00	1:00	1524.65	1524.63	1524.64	0.018	73.781	73.744	-0.037	-10.243	
62	Falgunn75	5	60	18:00	19:00	1:00	1524.64	1524.62	1524.63	0.02	73.76	73.719	-0.041	-11.379
63		6	60	18:00	19:00	1:00	1524.6	1524.58	1524.59	0.02	73.678	73.637	-0.041	-11.37
64		8	60	18:00	19:00	1:00	1524.61	1524.59	1524.6	0.018	73.699	73.662	-0.037	-10.236

Case	Month/Year	Date	Load	Machine Start	Machine Stop	Running Hour	Water level at Start	Water level at stop	Average Water Level	Change in water level	Volume of Water (10 ⁶ m ³) at Start	Volume of Water (10 ⁶ m ³) at Stop	Change of Reservoir	Change Rate
65		14	60	18:00	19:00	1:00	1524.6	1524.58	1524.59	0.021	73.678	73.635	-0.043	-11.939
66		17	60	18:00	19:00	1:00	1524.68	1524.66	1524.67	0.019	73.842	73.803	-0.039	-10.819
67		19	60	18:00	19:00	1:00	1524.69	1524.67	1524.68	0.02	73.863	73.822	-0.041	-11.39
68	Chaitra 75	1	60	18:00	19:00	1:00	1524.76	1524.74	1524.75	0.02	74.006	73.965	-0.041	-11.406
69		7	60	18:00	20:00	2:00	1524.78	1524.74	1524.76	0.04	74.047	73.965	-0.082	-11.408
70		8	60	18:00	19:00	1:00	1524.67	1524.65	1524.66	0.02	73.822	73.781	-0.041	-11.386
71		17	60	18:00	19:00	1:00	1524.38	1524.36	1524.37	0.02	73.229	73.188	-0.041	-11.322
72		18	60	18:00	20:00	2:00	1524.27	1524.23	1524.25	0.04	73.005	72.924	-0.081	-11.296
73		19	60	11:00	21:00	10:00	1524.15	1523.94	1524.05	0.21	72.761	72.336	-0.425	-11.814
74		21	60	10:00	15:00	5:00	1523.53	1523.43	1523.48	0.1	71.511	71.31	-0.2	-11.128
75	Poush 76	1	60	17:00	18:00	1:00	1520.98	1520.96	1520.97	0.023	66.524	66.48	-0.044	-12.18
76		4	60	8:00	9:00	1:00	1520.77	1520.75	1520.76	0.021	66.124	66.084	-0.04	-11.075
77		6	60	18:00	19:00	1:00	1520.64	1520.62	1520.63	0.023	65.877	65.834	-0.044	-12.098
78		7	60	18:00	20:00	2:00	1520.5	1520.46	1520.48	0.045	65.613	65.528	-0.085	-11.799
79		8	60	17:00	19:00	2:00	1520.34	1520.29	1520.32	0.05	65.311	65.217	-0.094	-13.068
80		9	60	8:00	11:00	3:00	1520.25	1520.19	1520.22	0.065	65.142	65.02	-0.122	-11.303
81		10	60	10:00	13:00	3:00	1520.02	1519.95	1519.99	0.07	64.71	64.58	-0.131	-12.116
82		11	60	7:00	9:00	2:00	1519.67	1519.63	1519.65	0.045	64.058	63.974	-0.084	-11.605

Case	Month/Year	Date	Load	Machine Start	Machine Stop	Running Hour	Water level at Start	Water level at stop	Average Water Level	Change in water level	Volume of Water (10 ⁶ m ³) at Start	Volume of Water (10 ⁶ m ³) at Stop	Change of Reservoir	Change Rate
83		13	60	10:00	12:00	2:00	1529.29	1529.25	1529.27	0.039	83.722	83.635	-0.087	-12.116
84		17	60	16:00	18:00	2:00	1518.74	1518.69	1518.72	0.049	62.346	62.257	-0.089	-12.401
85		26	60	7:30	11:00	3:30	1517.7	1517.62	1517.66	0.084	60.47	60.321	-0.15	-11.889
86		27	60	18:00	19:00	1:00	1517.5	1517.48	1517.49	0.025	60.114	60.07	-0.044	-12.342
87		28	60	18:00	19:00	1:00	1517.31	1517.29	1517.3	0.024	59.777	59.735	-0.042	-11.802
88	Magh 76	9	60	16:00	17:00	1:00	1517.88	1517.86	1517.87	0.022	60.792	60.753	-0.039	-10.946
89		10	60	8:00	9:00	1:00	1517.8	1517.78	1517.79	0.025	60.649	60.604	-0.045	-12.418
90		16	60	7:00	8:00	1:00	1517.2	1517.18	1517.19	0.025	59.582	59.538	-0.044	-12.266
91		21	60	8:00	9:00	1:00	1516.81	1516.79	1516.8	0.024	58.896	58.854	-0.042	-11.682
92	Chaitra 76	13	60	18:30	19:00	0:30	1514.99	1514.98	1514.98	0.013	55.765	55.743	-0.022	-12.189
93		14	60	18:00	19:00	1:00	1514.99	1514.97	1514.98	0.025	55.765	55.723	-0.042	-11.719
94		17	60	18:00	19:00	1:00	1514.98	1514.95	1514.97	0.026	55.748	55.705	-0.044	-12.185
95		18	60	18:30	19:00	0:30	1514.89	1514.88	1514.88	0.013	55.597	55.575	-0.022	-12.164
96		19	60	18:30	19:30	1:00	1514.76	1514.74	1514.75	0.025	55.378	55.336	-0.042	-11.663
97		20	60	19:00	20:00	1:00	1514.71	1514.68	1514.7	0.026	55.294	55.25	-0.044	-12.116
98		21	60	18:00	19:00	1:00	1514.54	1514.52	1514.53	0.025	55.009	54.968	-0.042	-11.609
99		23	60	8:00	12:00	4:00	1514.32	1514.22	1514.27	0.105	54.642	54.468	-0.175	-12.123
100		24	60	18:40	20:00	1:20	1513.92	1513.88	1513.9	0.037	53.979	53.918	-0.061	-12.718

Case	Month/Year	Date	Load	Machine Start	Machine Stop	Running Hour	Water level at Start	Water level at stop	Average Water Level	Change in water level	Volume of Water (10 ⁶ m ³) at Start	Volume of Water (10 ⁶ m ³) at Stop	Change of Reservoir	Change Rate
101		25	60	19:00	20:00	1:00	1513.72	1513.7	1513.71	0.025	53.65	53.609	-0.041	-11.411
102		28	60	7:00	10:00	3:00	1513.31	1513.23	1513.27	0.08	52.979	52.849	-0.13	-12.06
103		29	60	18:00	19:00	1:00	1512.9	1512.87	1512.89	0.028	52.314	52.268	-0.045	-12.561
104		30	60	18:00	19:00	1:00	1512.7	1512.67	1512.69	0.029	51.991	51.945	-0.047	-12.954
105	Poush77	1	60	17:00	18:00	1:00	1522.67	1522.65	1522.66	0.022	69.801	69.757	-0.043	-12.046
106		2	60	14:00	19:00	5:00	1522.53	1522.42	1522.48	0.11	69.525	69.309	-0.216	-12.002
107		3	60	14:00	21:00	7:00	1522.29	1522.13	1522.21	0.156	69.054	68.749	-0.305	-12.096
108		7	60	18:00	22:00	4:00	1521.6	1521.51	1521.55	0.095	67.713	67.53	-0.183	-12.724
109		8	60	11:00	19:00	8:00	1521.48	1521.31	1521.4	0.17	67.482	67.155	-0.327	-11.349
110		10	60	18:00	20:00	2:00	1521.14	1521.1	1521.12	0.045	66.829	66.743	-0.086	-11.95
111		14	60	16:00	20:00	4:00	1520.6	1520.51	1520.56	0.09	65.802	65.632	-0.17	-11.817
112		17	60	8:00	10:00	2:00	1520.03	1519.98	1520.01	0.046	64.729	64.643	-0.086	-11.948
113		18	60	15:00	21:00	6:00	1519.61	1519.47	1519.54	0.14	63.947	63.687	-0.259	-12.008
114		20	60	13:00	21:00	8:00	1519.4	1519.21	1519.31	0.19	63.558	63.207	-0.35	-12.165
115		24	60	16:00	20:00	4:00	1518.46	1518.36	1518.41	0.1	61.837	61.656	-0.181	-12.576
116		27	60	17:00	19:00	2:00	1518.12	1518.07	1518.09	0.051	61.223	61.131	-0.092	-12.745
117		28	60	13:00	19:00	6:00	1517.96	1517.81	1517.89	0.15	60.936	60.667	-0.269	-12.442
118		29	60	9:00	18:00	9:00	1517.74	1517.52	1517.63	0.22	60.542	60.15	-0.392	-12.103

Case	Month/Year	Date	Load	Machine Start	Machine Stop	Running Hour	Water level at Start	Water level at stop	Average Water Level	Change in water level	Volume of Water (10 ⁶ m ³) at Start	Volume of Water (10 ⁶ m ³) at Stop	Change of Reservoir	Change Rate
119	Magh 77	2	60	9:00	17:00	8:00	1517.46	1517.26	1517.36	0.2	60.043	59.689	-0.355	-12.31
120		3	60	7:30	9:00	1:30	1517.25	1517.21	1517.23	0.04	59.671	59.6	-0.071	-13.095
121		5	60	16:00	20:00	4:00	1516.94	1516.83	1516.89	0.11	59.124	58.931	-0.193	-13.41
122		6	60	12:00	15:00	3:00	1516.76	1516.68	1516.72	0.085	58.809	58.66	-0.149	-13.768
123		7	60	15:00	21:00	6:00	1516.45	1516.29	1516.37	0.16	58.267	57.99	-0.278	-12.866
124		8	60	17:00	19:00	2:00	1516.1	1516.04	1516.07	0.056	57.661	57.564	-0.097	-13.427
125		9	60	13:00	20:00	7:00	1515.92	1515.73	1515.83	0.19	57.35	57.024	-0.326	-12.949
126		12	60	18:00	20:00	2:00	1515.25	1515.19	1515.22	0.06	56.205	56.104	-0.102	-14.134
127		13	60	9:00	18:00	9:00	1515.15	1514.9	1515.03	0.25	56.036	55.614	-0.422	-13.034
128		14	60	9:00	18:00	9:00	1514.79	1514.54	1514.67	0.25	55.428	55.009	-0.419	-12.936
129		15	60	19:00	21:00	2:00	1514.28	1514.23	1514.26	0.05	54.576	54.493	-0.083	-11.543
130		16	60	19:00	22:00	3:00	1513.94	1513.86	1513.9	0.08	54.012	53.88	-0.132	-12.221
131		18	60	15:00	21:00	6:00	1513.65	1513.49	1513.57	0.16	53.535	53.273	-0.262	-12.137
132		19	60	10:00	20:00	10:00	1513.42	1513.13	1513.28	0.288	53.158	52.689	-0.469	-13.027
133		20	60	13:00	17:00	4:00	1512.99	1512.87	1512.93	0.116	52.459	52.272	-0.188	-13.022
134	21	60	15:00	17:00	2:00	1512.64	1512.58	1512.61	0.058	51.895	51.802	-0.093	-12.934	
135	Falgun 77	6	60	17:00	19:00	2:00	1511.75	1511.69	1511.72	0.059	50.478	50.386	-0.093	-12.909
136		14	60	6:30	9:00	2:30	1511.59	1511.52	1511.55	0.075	50.227	50.109	-0.118	-13.081

Case	Month/Year	Date	Load	Machine Start	Machine Stop	Running Hour	Water level at Start	Water level at stop	Average Water Level	Change in water level	Volume of Water (10 ⁶ m ³) at Start	Volume of Water (10 ⁶ m ³) at Stop	Change of Reservoir	Change Rate
137	Chaitra 77	1	60	12:15	17:32	5:17	1511.39	1511.23	1511.31	0.159	49.913	49.665	-0.248	-13.054
138		8	60	12:00	13:12	1:12	1511.1	1511.06	1511.08	0.038	49.461	49.402	-0.059	-13.669
139		10	60	18:00	21:00	3:00	1510.84	1510.74	1510.79	0.1	49.058	48.903	-0.154	-14.298
140		13	60	16:00	17:00	1:00	1510.27	1510.24	1510.25	0.035	48.182	48.129	-0.053	-14.84
141		16	60	17:00	18:00	1:00	1509.71	1509.68	1509.69	0.035	47.332	47.279	-0.053	-14.661
142		19	60	18:00	19:00	1:00	1509.34	1509.31	1509.32	0.035	46.776	46.724	-0.052	-14.544
143		20	60	18:30	20:00	1:30	1509.31	1509.26	1509.29	0.05	46.731	46.657	-0.075	-13.84
144		22	60	15:00	21:00	6:00	1509.22	1509.03	1509.13	0.189	46.597	46.315	-0.282	-13.033
145		23	60	10:00	21:00	11:00	1509	1508.65	1508.83	0.35	46.269	45.751	-0.518	-13.079
146		24	60	14:00	21:00	7:00	1508.54	1508.29	1508.42	0.25	45.589	45.223	-0.367	-14.549
147		25	60	17:00	23:00	6:00	1508.11	1507.89	1508	0.22	44.96	44.64	-0.32	-14.801
148		26	60	16:00	22:00	6:00	1507.63	1507.41	1507.52	0.22	44.264	43.948	-0.316	-14.645
149		27	60	18:00	19:00	1:00	1507.21	1507.18	1507.19	0.035	43.662	43.612	-0.05	-13.879
150		28	60	9:00	12:00	3:00	1507.17	1507.07	1507.12	0.1	43.605	43.462	-0.143	-13.197
151		29	60	10:00	23:00	13:00	1506.99	1506.54	1506.77	0.45	43.348	42.712	-0.636	-13.597
152		30	60	17:00	21:00	4:00	1506.29	1506.15	1506.22	0.14	42.361	42.166	-0.196	-13.582

Reservoir inflow during machine stop.

Table 5.5: Volume of water inflow during machine stop

Case	Month/Year	Date	Stop	Start	Duration	Water level at Stop	Water level at Start	Change in water level	Volume of Water (10 ⁶ m ³) at Start	Volume of Water (10 ⁶ m ³) at Stop	Volume Added	Addition Rate (m ³ /s)
1	Poush 73	26	1:00 AM	7:00 AM	6:00	1522.77	1522.78	0.01	70.00	70.02	0.02	0.91
2		27	1:00 AM	7:00 AM	6:00	1522.61	1522.62	0.01	69.68	69.70	0.02	0.91
3		29	1:00 AM	7:00 AM	6:00	1522.25	1522.26	0.01	68.98	69.00	0.02	0.91
4	Magh 73	2	1:00 AM	7:00 AM	6:00	1522.07	1522.08	0.01	68.62	68.64	0.02	0.90
5		6	2:00 AM	6:00 AM	4:00	1521.60	1521.61	0.01	67.71	67.73	0.02	1.34
6		7	1:00 AM	6:00 AM	5:00	1521.43	1521.44	0.01	67.39	67.40	0.02	1.07
7		12	1:00 AM	6:00 AM	5:00	1520.80	1520.81	0.01	66.18	66.20	0.02	1.06
8		16	1:00 AM	7:00 AM	6:00	1520.40	1520.41	0.01	65.42	65.44	0.02	0.87
9		23	1:00 AM	8:00 AM	7:00	1519.76	1519.78	0.02	64.23	64.26	0.04	1.48
10		27	1:00 AM	5:00 AM	4:00	1519.16	1519.17	0.01	63.12	63.13	0.02	1.28
11		29	1:00 AM	7:00 AM	6:00	1518.85	1518.87	0.02	62.55	62.58	0.04	1.69
12	Falgun 73	1	1:00 AM	6:00 AM	5:00	1518.68	1518.71	0.03	62.24	62.29	0.05	3.04
13		2	1:00 AM	5:00 AM	4:00	1518.58	1518.59	0.01	62.06	62.07	0.02	1.26

Case	Month/Year	Date	Stop	Start	Duration	Water level at Stop	Water level at Start	Change in water level	Volume of Water (10 ⁶ m ³) at Start	Volume of Water (10 ⁶ m ³) at Stop	Volume Added	Addition Rate (m ³ /s)
14		3	1:00 AM	5:00 AM	4:00	1518.39	1518.40	0.01	61.71	61.73	0.02	1.26
15		5	1:00 AM	7:00 AM	6:00	1517.94	1517.95	0.01	60.90	60.92	0.02	0.83
16		16	1:00 AM	7:00 AM	6:00	1516.38	1516.40	0.02	58.15	58.18	0.03	1.61
17		18	1:00 AM	5:00 AM	4:00	1515.95	1515.96	0.005	57.40	57.41	0.01	0.60
18		19	1:00 AM	6:00 AM	5:00	1515.74	1515.75	0.01	57.04	57.06	0.02	0.95
19		21	1:00 AM	5:00 AM	4:00	1515.41	1515.42	0.01	56.48	56.49	0.02	1.18
20		23	2:00 AM	5:00 AM	3:00	1515.02	1515.03	0.01	55.82	55.83	0.02	1.56
21		24	1:00 AM	5:00 AM	4:00	1514.76	1514.77	0.01	55.38	55.39	0.02	1.17
22	Chaitra 73	3	1:00 AM	6:00 AM	5:00	1513.72	1513.73	0.01	53.65	53.67	0.02	0.91
23		4	1:00 AM	6:00 AM	5:00	1513.51	1513.53	0.02	53.31	53.34	0.03	1.82
24		6	1:00 AM	8:00 AM	7:00	1513.34	1513.36	0.02	53.03	53.06	0.03	1.29
25		8	1:00 AM	7:00 AM	6:00	1512.95	1512.97	0.02	52.39	52.43	0.03	1.50
26		25	1:00 PM	6:00 PM	5:00	1511.17	1511.19	0.02	49.57	49.60	0.03	1.73
27		26	1:00 AM	7:00 AM	6:00	1511.09	1511.11	0.02	49.45	49.48	0.03	1.44
28		27	1:00 AM	5:00 AM	4:00	1510.85	1510.86	0.01	49.07	49.09	0.02	1.07

Case	Month/Year	Date	Stop	Start	Duration	Water level at Stop	Water level at Start	Change in water level	Volume of Water (10 ⁶ m ³) at Start	Volume of Water (10 ⁶ m ³) at Stop	Volume Added	Addition Rate (m ³ /s)
29		28	1:00 AM	9:00 AM	8:00	1509.76	1509.78	0.02	47.41	47.44	0.03	1.05
30	Poush 74	19	1:00 AM	9:00 AM	8:00	1524.35	1524.37	0.02	73.17	73.21	0.04	1.41
31		25	1:00 AM	8:00 AM	7:00	1524.01	1524.02	0.01	72.48	72.50	0.02	0.80
32		26	1:00 AM	7:00 AM	6:00	1523.83	1523.85	0.02	72.11	72.15	0.04	1.87
33	Magh 74	12	1:00 AM	9:00 AM	8:00	1523.25	1523.27	0.02	70.95	70.99	0.04	1.39
34	Chaitra 74	5	1:00 AM	9:00 AM	8:00	1523.25	1523.27	0.02	70.95	70.99	0.04	1.39
35		6	1:00 AM	12:00 PM	11:00	1514.04	1514.07	0.03	54.18	54.23	0.05	1.25
36		12	1:00 AM	12:00 PM	11:00	1513.81	1513.85	0.04	53.80	53.86	0.07	1.66
37		13	1:00 AM	12:00 PM	11:00	1513.95	1513.98	0.03	54.03	54.08	0.05	1.25
38		26	1:00 AM	4:00 AM	3:00	1512.56	1512.57	0.01	51.77	51.78	0.02	1.49
39	Poush 75	2	1:00 AM	1:00 PM	12:00	1526.50	1526.51	0.01	77.64	77.66	0.02	0.49
40		10	1:00 AM	8:00 AM	7:00	1526.43	1526.44	0.01	77.49	77.51	0.02	0.84
41		11	1:00 AM	5:00 PM	16:00	1526.39	1526.40	0.01	77.41	77.43	0.02	0.37
42		12	1:00 AM	5:00 PM	16:00	1526.35	1526.37	0.02	77.32	77.36	0.04	0.74

Case	Month/Year	Date	Stop	Start	Duration	Water level at Stop	Water level at Start	Change in water level	Volume of Water (10 ⁶ m ³) at Start	Volume of Water (10 ⁶ m ³) at Stop	Volume Added	Addition Rate (m ³ /s)
43		13	1:00 AM	9:00 AM	8:00	1526.29	1526.30	0.01	77.19	77.22	0.02	0.73
44		15	1:00 AM	6:00 PM	17:00	1526.25	1526.26	0.01	77.11	77.13	0.02	0.35
45		16	1:00 AM	9:00 AM	8:00	1526.21	1526.22	0.01	77.03	77.05	0.02	0.73
46		17	1:00 AM	8:00 AM	7:00	1526.14	1526.15	0.01	76.88	76.90	0.02	0.84
47		18	1:00 AM	6:00 PM	17:00	1526.08	1526.09	0.01	76.75	76.77	0.02	0.34
48		19	1:00 AM	8:00 AM	7:00	1526.04	1526.06	0.02	76.67	76.71	0.04	1.67
49		20	1:00 AM	7:00 PM	18:00	1525.94	1525.95	0.01	76.46	76.48	0.02	0.09
50		22	1:00 AM	8:00 AM	7:00	1525.75	1525.77	0.02	76.06	76.10	0.04	1.66
51		23	1:00 AM	8:00 AM	7:00	1525.65	1525.67	0.02	75.85	75.89	0.04	1.66
52		25	1:00 AM	7:00 AM	6:00	1525.50	1525.51	0.01	75.54	75.56	0.02	0.96
53		26	1:00 AM	8:00 AM	7:00	1525.44	1525.46	0.02	75.41	75.45	0.04	1.65
54	Magh 75	9	1:00 AM	6:00 PM	17:00	1525.02	1525.06	0.04	74.54	74.62	0.08	1.35
55		14	1:00 AM	12:00 PM	11:00	1525.04	1525.05	0.01	74.58	74.60	0.02	0.52
56		15	1:00 AM	7:00 AM	6:00	1525.00	1525.01	0.01	74.50	74.52	0.02	0.96
57		17	1:00 AM	8:00 AM	7:00	1524.83	1524.85	0.02	74.15	74.19	0.04	1.63

Case	Month/Year	Date	Stop	Start	Duration	Water level at Stop	Water level at Start	Change in water level	Volume of Water (10 ⁶ m ³) at Start	Volume of Water (10 ⁶ m ³) at Stop	Volume Added	Addition Rate (m ³ /s)
58		18	1:00 AM	8:00 AM	7:00	1524.72	1524.73	0.01	73.92	73.94	0.02	0.81
59		19	1:00 AM	8:00 AM	7:00	1524.63	1524.64	0.01	73.74	73.76	0.02	0.81
60		26	1:00 AM	6:00 PM	17:00	1524.41	1524.46	0.05	73.29	73.39	0.10	1.67
61		29	1:00 AM	7:00 AM	6:00	1524.63	1524.65	0.02	73.74	73.78	0.04	1.90
62	Falgunn75	5	1:00 AM	8:00 AM	7:00	1524.62	1524.63	0.01	73.72	73.74	0.02	0.81
63		6	1:00 AM	7:00 AM	6:00	1524.61	1524.62	0.01	73.70	73.72	0.02	0.95
64		8	1:00 AM	5:00 PM	16:00	1524.56	1524.61	0.05	73.60	73.70	0.10	1.78
65		14	1:00 AM	7:00 PM	18:00	1524.58	1524.59	0.01	73.64	73.66	0.02	0.32
66		17	1:00 AM	8:00 AM	7:00	1524.66	1524.68	0.02	73.80	73.84	0.04	1.63
67		19	1:00 AM	6:00 PM	17:00	1524.66	1524.69	0.03	73.80	73.86	0.06	1.00
68	Chaitra 75	1	1:00 AM	7:00 AM	6:00	1524.76	1524.77	0.01	74.01	74.03	0.02	0.95
69		7	1:00 AM	8:00 AM	7:00	1524.78	1524.79	0.01	74.05	74.07	0.02	0.82
70		8	1:00 AM	8:00 AM	7:00	1524.74	1524.75	0.01	73.97	73.99	0.02	0.81
71		17	1:00 AM	8:00 AM	7:00	1524.38	1524.39	0.01	73.23	73.25	0.02	0.81
72		18	1:00 AM	6:00 AM	5:00	1524.36	1524.37	0.01	73.19	73.21	0.02	1.13

Case	Month/Year	Date	Stop	Start	Duration	Water level at Stop	Water level at Start	Change in water level	Volume of Water (10 ⁶ m ³) at Start	Volume of Water (10 ⁶ m ³) at Stop	Volume Added	Addition Rate (m ³ /s)
73		19	1:00 AM	6:00 AM	5:00	1524.20	1524.21	0.01	72.86	72.88	0.02	1.13
74		21	9:00 AM	1:00 PM	4:00	1523.64	1523.65	0.01	71.73	71.75	0.02	1.40
75	Poush 76	1	1:00 AM	8:00 AM	7:00	1521.03	1521.04	0.01	66.62	66.64	0.02	0.76
76		4	1:00 AM	7:00 AM	6:00	1520.75	1520.77	0.02	66.09	66.12	0.04	1.76
77		6	1:00 AM	8:00 AM	7:00	1520.67	1520.68	0.01	65.93	65.95	0.02	0.75
78		7	1:00 AM	7:00 AM	6:00	1520.60	1520.61	0.01	65.80	65.82	0.02	0.88
79		8	1:00 AM	7:00 AM	6:00	1520.44	1520.45	0.01	65.50	65.52	0.02	0.87
80		9	1:00 AM	7:00 AM	6:00	1520.25	1520.27	0.02	65.14	65.18	0.04	1.74
81		10	1:00 AM	7:00 AM	6:00	1520.04	1520.05	0.01	64.75	64.77	0.02	0.87
82		11	1:00 AM	7:00 AM	6:00	1519.82	1519.83	0.01	64.34	64.36	0.02	0.86
83		13	1:00 AM	8:00 AM	7:00	1519.57	1519.58	0.01	63.87	63.89	0.02	0.74
84		17	1:00 AM	8:00 AM	7:00	1518.80	1518.81	0.01	62.46	62.47	0.02	0.72
85		26	1:00 AM	8:00 AM	7:00	1517.68	1517.69	0.01	60.43	60.45	0.02	0.71
86		27	1:00 AM	7:00 AM	6:00	1517.60	1517.61	0.01	60.29	60.31	0.02	0.82
87		28	1:00 AM	8:00 AM	7:00	1517.44	1517.46	0.02	60.01	60.04	0.04	1.41

Case	Month/Year	Date	Stop	Start	Duration	Water level at Stop	Water level at Start	Change in water level	Volume of Water (10 ⁶ m ³) at Start	Volume of Water (10 ⁶ m ³) at Stop	Volume Added	Addition Rate (m ³ /s)
88	Magh 76	9	2:00 AM	7:00 AM	5:00	1517.94	1517.96	0.02	60.90	60.94	0.04	1.99
89		10	1:00 AM	7:00 AM	6:00	1517.80	1517.81	0.01	60.65	60.67	0.02	0.83
90		16	1:00 AM	7:00 AM	6:00	1517.19	1517.20	0.01	59.56	59.58	0.02	0.82
91		21	1:00 AM	7:00 AM	6:00	1516.80	1516.82	0.02	58.88	58.91	0.04	1.62
92	Chaitra 76	13	1:00 AM	7:00 PM	18:00	1514.95	1514.98	0.03	55.70	55.75	0.05	0.78
93		14	1:00 AM	9:00 AM	8:00	1514.97	1514.99	0.02	55.73	55.77	0.03	1.17
94		17	1:00 AM	8:00 AM	7:00	1514.97	1514.98	0.01	55.73	55.75	0.02	0.67
95		18	1:00 AM	8:00 AM	7:00	1514.95	1514.96	0.01	55.70	55.71	0.02	0.67
96		19	1:00 AM	7:00 AM	6:00	1514.84	1514.86	0.02	55.51	55.55	0.03	1.56
97		20	1:00 AM	8:00 AM	7:00	1514.71	1514.72	0.01	55.29	55.31	0.02	0.67
98		21	1:00 AM	9:00 AM	8:00	1514.64	1514.67	0.03	55.18	55.23	0.05	1.75
99		23	2:00 AM	7:00 AM	5:00	1514.32	1514.33	0.01	54.64	54.66	0.02	0.92
100		24	1:00 AM	8:00 AM	7:00	1514.04	1514.05	0.01	54.18	54.19	0.02	0.66
101		25	1:00 AM	7:00 AM	6:00	1513.84	1513.86	0.02	53.85	53.88	0.03	1.53
102		28	1:00 AM	8:00 AM	7:00	1513.30	1513.31	0.01	52.96	52.98	0.02	0.65

Case	Month/Year	Date	Stop	Start	Duration	Water level at Stop	Water level at Start	Change in water level	Volume of Water (10 ⁶ m ³) at Start	Volume of Water (10 ⁶ m ³) at Stop	Volume Added	Addition Rate (m ³ /s)
103		29	1:00 AM	5:00 AM	4:00	1513.04	1513.05	0.01	52.54	52.56	0.02	1.13
104		30	1:00 AM	8:00 AM	7:00	1512.82	1512.83	0.01	52.18	52.20	0.02	0.64
105	Poush77	1	1:00 AM	6:00 AM	5:00	1522.75	1522.76	0.01	69.96	69.98	0.02	1.10
106		2	1:00 AM	7:00 AM	6:00	1522.61	1522.63	0.02	69.68	69.72	0.04	1.82
107		3	1:00 AM	7:00 AM	6:00	1522.38	1522.40	0.02	69.23	69.27	0.04	1.82
108		7	1:00 AM	8:00 AM	7:00	1521.60	1521.61	0.01	67.71	67.73	0.02	0.77
109		8	1:00 AM	7:00 AM	6:00	1521.51	1521.53	0.02	67.54	67.58	0.04	1.78
110		10	1:00 AM	7:00 AM	6:00	1521.19	1521.20	0.01	66.92	66.94	0.02	0.89
111		14	2:00 AM	7:00 AM	5:00	1520.74	1520.75	0.01	66.07	66.09	0.02	1.05
112		17	1:00 AM	6:00 AM	5:00	1520.03	1520.04	0.01	64.73	64.75	0.02	1.04
113		18	1:00 AM	8:00 AM	7:00	1519.80	1519.82	0.02	64.30	64.34	0.04	1.48
114		20	1:00 AM	7:00 AM	6:00	1519.46	1519.48	0.02	63.67	63.71	0.04	1.71
115		24	2:00 AM	7:00 AM	5:00	1519.54	1519.55	0.01	63.82	63.84	0.02	1.03
116		27	1:00 AM	8:00 AM	7:00	1518.22	1518.24	0.02	61.40	61.44	0.04	1.43
117	28	1:00 AM	8:00 AM	7:00	1518.00	1518.02	0.015	61.01	61.03	0.03	1.07	

Case	Month/Year	Date	Stop	Start	Duration	Water level at Stop	Water level at Start	Change in water level	Volume of Water (10 ⁶ m ³) at Start	Volume of Water (10 ⁶ m ³) at Stop	Volume Added	Addition Rate (m ³ /s)
118		29	1:00 AM	6:00 AM	5:00	1517.73	1517.74	0.01	60.52	60.54	0.02	0.99
119	Magh 77	2	1:00 AM	8:00 AM	7:00	1517.44	1517.46	0.02	60.01	60.04	0.04	1.41
120		3	1:00 AM	9:00 AM	8:00	1517.21	1517.22	0.01	59.60	59.62	0.02	0.61
121		5	1:00 AM	7:00 AM	6:00	1517.03	1517.04	0.01	59.28	59.30	0.02	0.82
122		6	1:00 AM	7:00 AM	6:00	1516.81	1516.82	0.01	58.90	58.91	0.02	0.81
123		7	1:00 AM	7:00 AM	6:00	1516.57	1516.58	0.01	58.48	58.49	0.02	0.81
124		8	1:00 AM	7:00 AM	6:00	1516.27	1516.28	0.01	57.95	57.97	0.02	0.80
125		9	1:00 AM	7:00 AM	6:00	1515.98	1515.99	0.01	57.45	57.47	0.02	0.80
126		12	1:00 AM	8:00 AM	7:00	1515.43	1515.44	0.01	56.51	56.53	0.02	0.68
127		13	1:00 AM	7:00 AM	6:00	1515.16	1515.17	0.01	56.05	56.07	0.02	0.78
128		14	1:00 AM	7:00 AM	6:00	1514.81	1514.82	0.01	55.46	55.48	0.02	0.78
129		15	1:00 AM	7:00 AM	6:00	1514.40	1514.42	0.02	54.78	54.81	0.03	1.54
130		16	1:00 AM	6:00 AM	5:00	1514.19	1514.20	0.01	54.43	54.44	0.02	0.92
131		18	1:00 AM	7:00 AM	6:00	1513.78	1513.80	0.02	53.75	53.78	0.03	1.52
132		19	1:00 AM	6:00 AM	5:00	1513.46	1513.47	0.01	53.22	53.24	0.02	0.91

Case	Month/Year	Date	Stop	Start	Duration	Water level at Stop	Water level at Start	Change in water level	Volume of Water (10 ⁶ m ³) at Start	Volume of Water (10 ⁶ m ³) at Stop	Volume Added	Addition Rate (m ³ /s)
133		20	1:00 AM	7:00 AM	6:00	1513.10	1513.11	0.013	52.64	52.66	0.02	0.98
134		21	1:00 AM	6:00 AM	5:00	1512.78	1512.79	0.01	52.12	52.14	0.02	0.90
135	Falgun 77	6	1:00 AM	7:00 AM	6:00	1511.80	1511.82	0.02	50.56	50.59	0.03	1.46
136		14	1:00 AM	7:00 AM	6:00	1511.58	1511.59	0.01	50.21	50.23	0.02	0.73
137	Chaitra 77	1	1:00 AM	1:00 PM	12:00	1511.36	1511.37	0.01	49.87	49.88	0.02	0.36
138		8	1:00 AM	1:00 PM	12:00	1511.08	1511.09	0.01	49.43	49.45	0.02	0.36
139		10	1:00 AM	7:00 AM	6:00	1510.91	1510.92	0.01	49.17	49.18	0.02	0.72
140		13	1:00 AM	8:00 AM	7:00	1510.38	1510.39	0.01	48.35	48.37	0.02	0.61
141		16	1:00 AM	8:00 AM	7:00	1509.78	1509.79	0.01	47.44	47.45	0.02	0.60
142		19	1:00 AM	11:00 AM	10:00	1509.45	1509.46	0.01	46.94	46.96	0.02	0.42
143		20	1:00 AM	4:00 PM	15:00	1509.30	1509.33	0.03	46.72	46.76	0.04	0.83
144		22	1:00 AM	7:00 PM	18:00	1509.21	1509.24	0.03	46.58	46.63	0.04	0.69
145		23	1:00 AM	7:00 AM	6:00	1509.03	1509.04	0.01	46.31	46.33	0.01	0.69
146		24	1:00 AM	7:00 AM	6:00	1505.65	1505.66	0.01	41.47	41.49	0.01	0.64
147	25	1:00 AM	7:00 AM	6:00	1508.27	1508.28	0.01	45.19	45.21	0.01	0.68	

Case	Month/Year	Date	Stop	Start	Duration	Water level at Stop	Water level at Start	Change in water level	Volume of Water (10 ⁶ m ³) at Start	Volume of Water (10 ⁶ m ³) at Stop	Volume Added	Addition Rate (m ³ /s)
148		26	2:00 AM	6:00 AM	4:00	1507.88	1507.89	0.01	44.63	44.64	0.01	1.01
149		27	1:00 AM	6:00 AM	5:00	1507.41	1507.42	0.01	43.95	43.96	0.01	0.80
150		28	1:00 AM	10:00 AM	9:00	1507.15	1507.17	0.02	43.58	43.60	0.03	0.88
151		29	1:00 AM	9:00 AM	8:00	1507.00	1507.02	0.02	43.36	43.39	0.03	0.99
152		30	3:00 AM	8:00 AM	5:00	1506.51	1506.53	0.02	42.67	42.70	0.03	1.56

APPENDIX B: DRAWING OF PELTON RUNNER BUCKET

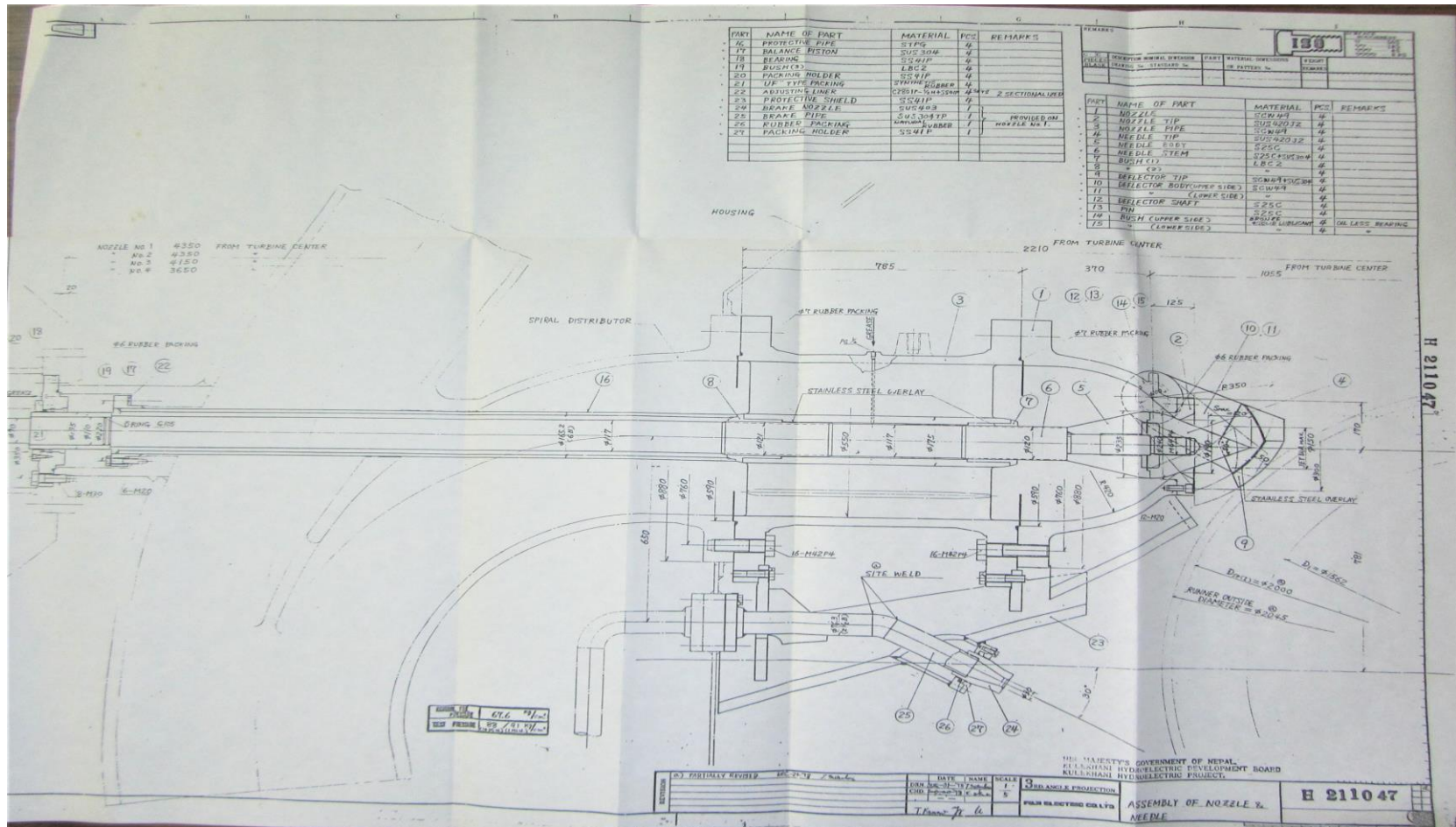


Figure 5.2: Nozzle and Needle

APPENDIX C: LABORATORY TEST REPORT



1. SEDIMENT CONCENTRATION ANALYSIS

Sediment Concentration Analysis was carried out at the site location. Weighing the original water sample, then carrying out the filtration; followed by drying and again weighing dry sample and hence calculating the ppm were the procedures which was followed by our technicians. Standard filtration method was adopted for sediment concentration analysis. The filtration paper used for the analysis was of 11-micron capacity. The concentration analysis was carried out in the laboratory in the site itself.

Measurement No	Date	Time	Sediment Concentration (ppm)	Remarks
0	2078/03/21	11:00 AM	48	Only Unit-1 running
1+4	2078/04/05	02:00 PM	70	Unit-1 & Unit-2 running
2	2078/04/06	11:00 AM	292	Both Unit Shut-Down
3	2078/04/06	03:00 PM	68	Only Unit-2 running

2. MINERAL CONTENT ANALYSIS

Scope

Erosion of hydro turbine components due to sediment content in water is a huge problem encountered by hydro power plants situated in the Himalayan region. Fine sand and silt particles carried by water cause abrasive wear and the rate of abrasion (erosion rate coefficient) depends on the hardness of parent material (i.e. metallic components of turbine), concentration of the particles, their grain size, shape and their hardness, velocity of the particles and their angle of impact. According to the literatures on abrasive wear in hydraulic machinery by Truscott, 1972, and Bergeron, 1950, in general, the absolute wear rate increases with grain size and sharpness. The intensity of erosion is directly proportional to the size of the particles; particle sizes above 200 to 250 μm are extremely harmful. It has been found that large size sediment particles (above 250 μm) even with hardness lesser than 5 on Mohs scale cause wear. Similarly, fine silt even with size less than 50 to 75 μm , containing quartz wears out the underwater parts. Thus, mineral content analysis helps to determine the proportion, and hardness of abrasive minerals in the sediment.

The samples were transported to Kathmandu and mineral Content Analysis was conducted using zoom stereo type microscope by manual observation method. Each sample was divided into four sets and analyzed separately and then average of the individual readings was calculated to identify the mineral content of that sample.



Apparatus

- Trinocular Stereo Zoom Microscope (for high magnification)
- Glass-slide
- Bench HCl (to detect carbonate minerals which are often difficult to recognize because of indistinct crystal form in their incomplete/broken state)
- Pointed needle (to separate overlapped mineral grains during grain-count, to supply acid at the required region in the field of view, as well as to distinguish platy and tabular grains in some instances)

Procedure

- The oven dried sample was spread on a glass slide, and remaining debris and organic matters were removed.
- Four observations for each sample were performed so that average of those results could be obtained as final result.
- Average amount of each mineral constituent was calculated in percentage, and tabulated along with their hardness number.

Results

Percentage of each mineral component in given sample was calculated and tabulated (**Table 1**) and averages also shown in pie chart (**Figure 1**).

Table 1: Mineral contents of sample number 1

Mineral	Percentage of various mineral grains					Mohs' Hardness	
	Observation 1	Observation 2	Observation 3	Observation 4	Average		
Quartz	64	60	71	57	63	7	
Feldspar	20	29	16	21	21.5	6	
Mica	8	5	4	14	7.75	2.5 - 3	
Other	A	6	3	5	2	4	≥5
	B	2	3	4	6	3.75	<5

• **Note:**

Other A: Tourmaline, Hornblende, and other hard rock fragments

Other B: Calcite, clay lumps, highly weathered soft rock fragments, and few unidentified sediments

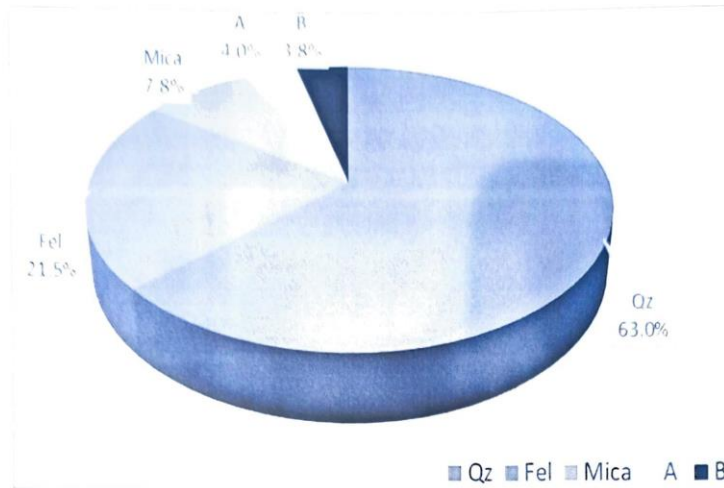


Figure 1: Diagram showing the percentage of average mineral constituents in samples

Conclusion

Hence, 88.5 percent of the mineral grains in the sediment contains minerals with hardness greater than 5 in Mohs' hardness scale which are Quartz, Feldspar, Tourmaline (1.8%), Hornblende (0.6%) and other hard minerals/rock fragments (~1.4%) as shown in **Figure 1**. Hence, they can abrade the turbine material. Remaining 11.5 percent of material comprises Mica (7.8%), calcite (0.9%), clay lumps, highly weathered rock fragments, etc. which possess hardness lower than 5 in Mohs' scale.

3. PARTICLE SIZE DISTRIBUTION (PSD) ANALYSIS

The samples collected from the site were transported to the head office and carried out PSD test by laser diffraction method using Beckman Coulter Particle Size Analyzer of capacity range of 0.4 micron to 2,000 microns. Laser diffraction method uses the scattering pattern of laser beam to determine the particle size of the sediment samples. The standard procedure provided by the equipment manufacturer was adopted for conducting the PSD analysis.

Standard approach was used for all laboratory works.





RESULT SHEET OF LABORATORY ANALYSES

Client:			
Project:	Kulekhani Hydropower Project		
Sampling location:	Project site		
Sample provided by:	Client		
Reporting date:	14 September 2021 (Lot 1)	Report no.:	250-29.L1

Type of analyses

SN	Types of Test	Qty	SN	Types of Test	Qty
A.	Suspended sediment concentration	-	B.	Particle size distribution (PSD)	√ 1
C.	Mineral content	-	D.	Organic matters content	-

B. Results of Particle Size Distribution (PSD)

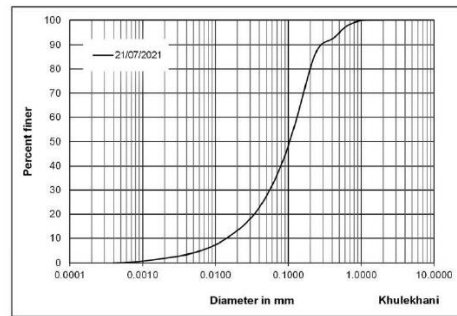


Figure B- 1: PSD curve of sample taken on 21 July 2021





File ID:	Kulekhani HPP	File ID:	Kulekhani HPP	File ID:	Kulekhani HPP
Sample ID:	SN 1	Sample ID:	SN 1	Sample ID:	SN 1
Comment 1:	21/07/2021	Comment 1:	21/07/2021	Comment 1:	21/07/2021
PSD:	1	PSD:	1	PSD:	1
Diameter in mm	Percent finer	Diameter in mm	Percent finer	Diameter in mm	Percent finer
0.00039	0	0.02382	15.0879	1.44293	100
0.00043	0.0149787	0.02615	16.2197	1.58398	100
0.00047	0.0416247	0.02870	17.4488	1.73886	100
0.00052	0.0811104	0.03151	18.7863	1.90887	100
0.00057	0.137961	0.03459	20.2449	2.00000	100
0.00063	0.209871	0.03797	21.8399		
0.00069	0.295619	0.04168	23.587		
0.00076	0.394552	0.04576	25.4982		
0.00083	0.506869	0.05023	27.5792		
0.00091	0.631375	0.05514	29.8288		
0.00100	0.766505	0.06053	32.244		
0.00110	0.910814	0.06645	34.8248		
0.00120	1.06308	0.07294	37.5793		
0.00132	1.2223	0.08007	40.5233		
0.00145	1.38691	0.08790	43.6779		
0.00159	1.55555	0.09649	47.0634		
0.00175	1.72709	0.10593	50.6941		
0.00192	1.90129	0.11629	54.5761		
0.00211	2.07789	0.12766	58.7057		
0.00231	2.25698	0.14013	63.065		
0.00254	2.43907	0.15383	67.6079		
0.00279	2.62554	0.16887	72.2375		
0.00306	2.81849	0.18538	76.7853		
0.00336	3.02046	0.20350	81.0127		
0.00369	3.23452	0.22340	84.6513		
0.00405	3.46404	0.24524	87.4808		
0.00444	3.71306	0.26922	89.4206		
0.00488	3.98591	0.29553	90.5931		
0.00535	4.28718	0.32443	91.2833		
0.00588	4.62109	0.35615	91.7907		
0.00645	4.99169	0.39097	92.353		
0.00708	5.40296	0.42918	93.1339		
0.00778	5.85855	0.47114	94.1765		
0.00854	6.36179	0.51720	95.3657		
0.00937	6.91485	0.56776	96.5125		
0.01029	7.5192	0.62327	97.472		
0.01129	8.17494	0.68420	98.2073		
0.01240	8.88138	0.75109	98.7613		
0.01361	9.63562	0.82452	99.1996		
0.01494	10.4333	0.90513	99.5568		
0.01640	11.2702	0.99359	99.8131		
0.01800	12.1457	1.09071	99.9502		
0.01976	13.0655	1.19740	99.9931		
0.02170	14.0412	1.31447	99.9997		